



Research paper

Discovery of indoximod prodrugs and characterization of clinical candidate NLG802

Sanjeev Kumar^a, Firoz A. Jaipuri^a, Jesse P. Waldo^a, Hima Potturi^a, Agnieszka Marciniowicz^a, James Adams^a, Clarissa Van Allen^a, Hong Zhuang^a, Nicholas Vahanian^a, Charles Link Jr.^a, Erik L. Brincks^{a, b, *}, Mario R. Mautino^a

^a NewLink Genetics, Ames, IA, 50010, United States

^b Lumos Pharma, Inc., Ames, IA, 50010, United States

ARTICLE INFO

Article history:

Received 2 March 2020

Received in revised form

20 April 2020

Accepted 21 April 2020

Available online 1 May 2020

Keywords:

Indoximod

Prodrugs

Drug exposure

Indoleamine 2,3-dioxygenase (IDO)

Amino acids

ABSTRACT

A series of different prodrugs of indoximod, including esters and peptide amides were synthesized with the aim of improving its oral bioavailability in humans. The pharmacokinetics of prodrugs that were stable in buffers, plasma and simulated gastric and intestinal fluids was first assessed in rats after oral dosing in solution or in capsule formulation. Two prodrugs that produced the highest exposure to indoximod in rats were further tested in Cynomolgus monkeys, a species in which indoximod has oral bioavailability of 6–10% and an equivalent dose-dependent exposure profile as humans. **NLG802** was selected as the clinical development candidate after increasing oral bioavailability (>5-fold), C_{max} (6.1–3.6 fold) and AUC (2.9–5.2 fold) in monkeys, compared to equivalent molar oral doses of indoximod. **NLG802** is extensively absorbed and rapidly metabolized to indoximod in all species tested and shows a safe toxicological profile at the anticipated therapeutic doses. **NLG802** markedly enhanced the anti-tumor responses of tumor-specific pmel-1 T cells in a melanoma tumor model. In conclusion, **NLG802** is a prodrug of indoximod expected to increase clinical drug exposure to indoximod above the current achievable levels, thus increasing the possibility of therapeutic effects in a larger fraction of the target patient population.

© 2020 The Authors. Published by Elsevier Masson SAS. This is an open access article under the CC BY license (<http://creativecommons.org/licenses/by/4.0/>).

1. Introduction

Indoximod (1-methyl-D-tryptophan, D1Mt, **1**) is an inhibitor of the indoleamine 2,3-dioxygenase (IDO) pathway, a cytosolic enzyme that catalyzes the oxidation of L-tryptophan (Trp) into N-formyl kynurenine (Kyn). The IDO pathway is a counter-regulatory mechanism that contributes to local control of inflammation and participates in creation of acquired peripheral tolerance in normal and pathological scenarios [1]. IDO-expressing cells are found constitutively in many tissues, including epididymis, gut, lymph nodes, spleen, thymus and lungs. In these tissues IDO regulates local inflammation and immune response to foreign or uncommon non-pathological antigens. IDO activity is also found at the maternal–fetal interface where it has a critical role in inducing

maternal immune tolerance to the paternally-derived allogeneic antigens expressed by the fetus [2–5]. The IDO pathway is induced in tumor cells and by host immune cells and contributes to acquired immunologic tolerance towards many types of tumors [6,7]. IDO expression by tumor cells has been demonstrated in melanoma, leukemia, pancreatic, ovarian, colorectal, endometrial and prostate cancers, and its expression is associated with significantly worse clinical outcomes [8–15]. IDO can also be expressed by cells of the host immune system that are associated with tumors [16]. In addition to IDO, the functionally analogous enzyme tryptophan 2,3-dioxygenase (TDO), which is mainly expressed in the liver, also participates in the degradation of Trp to Kyn and potentially provides a redundant or compensatory function to IDO in the creation of local tolerance to tumors. In fact, TDO is highly expressed in human glioblastoma tumors and other tumor cell lines [17], and its inhibition in TDO-expressing tumor models enhances antitumor activity [18]. Thus, the TDO pathway is also a potential player in the creation of local tolerance to tumors by Trp degradation.

The activities of the IDO and TDO enzymes result in reduction of

* Corresponding author. Lumos Pharma, Inc., 2503 S Loop Dr, Bldg 5, Suite 5100, Ames, IA, 50010, USA.

E-mail address: ebrincks@lumos-pharma.com (E.L. Brincks).

Trp and increase in Kyn levels, Low levels of Trp activate the General Control Nonrepressed-2 (GCN2) pathway [19,20], which leads to the creation of a Trp insufficiency signal that inactivates MAP4K3/GLK and mTOR [21]. Additionally, high Kyn levels (and its downstream metabolites) are sensed by the Aryl Hydrocarbon Receptor (AhR), a ligand-activated transcription factor that controls the expression of several genes involved in control of the immune response, such as *IDO1*, *FOXP3* and *RORC* [22–28]. The combination of these signals has significant downstream effects on the phenotype and function of immune cells such as dendritic cells (DCs), effector CD8⁺ T cells, CD4⁺ helper and regulatory T cells (Tregs), leading to a generalized immunosuppressive response.

Indoximod is an inhibitor of the IDO/TDO pathway, but it is fundamentally different from other selective or dual IDO/TDO inhibitors in that it does not directly inhibit the enzymatic activity of IDO or TDO, but instead opposes the effects elicited by these enzymes. Indoximod has a unique multi-faceted mechanism of action based on reactivation of mTOR and on the modulation of AhR function [21,29]. These effects are independent on the Trp metabolizing activity of IDO or TDO but oppose the effects of the enzymatic activity of both IDO and TDO. First, indoximod creates a Trp-sufficiency signal which leads to reactivation of MAP4K3 and subsequent activation of mTORC1 activity, thus opposing and bypassing the effects of Trp deprivation that lead to GCN2 activation and MAP4K3 and mTOR inactivation. This effect requires a relatively high concentration of indoximod (approximately 20 μM under normal Trp levels and 45 μM under low Trp conditions), is observed in both CD4⁺ and CD8⁺ T cells and leads to an increase in the proliferative capacity of activated effector and helper T cells [29]. Second, indoximod skews the differentiation program of primary CD4⁺ T cells, favoring a TH17 helper phenotype while inhibiting a regulatory phenotype by modulating the activity of AhR, a transcription factor which in the presence of Kyn or other ligands has the opposite effects [29]. Indoximod induces the transcription of *RORC* mRNA and represses the transcription of *FOXP3* mRNA. This pharmacodynamic effect takes place at clinically relevant concentrations of indoximod (EC_{90} of 10 μM) and is independent of IDO/TDO activity or exogenous Kyn, though it happens to oppose the Kyn/AhR effects on T cell differentiation [29]. Third, indoximod can downregulate IDO1 protein expression in human CD11c⁺CD123⁺CD83⁺ DCs (moDCs), and in murine IDO⁺ plasmacytoid DCs (pDCs) in tumor-draining lymph nodes (TDLN) [29]. These effects are observed with potency of approximately 30 μM , via a mechanism that involves the function of AhR. This direct modulation of IDO protein expression exerts inhibition on the IDO pathway by blocking both the enzymatic and non-enzymatic signaling functions of IDO1 that contribute to modulation of T cell function. In fact, mixed-lymphocyte response (MLR) T cell proliferation assays of both human or murine origin show that T cells that are in an IDO⁺ environment restore proliferative activity at concentrations of indoximod higher than 40 μM .

The therapeutic concentration requirements of indoximod have been established using in murine tumor models. In this setting, biological effects of indoximod are observed when mice are dosed at 62 mg/kg bid, which results in a daily exposure for indoximod ($\text{AUC}_{0-24\text{h,ss}}$) > 170 $\mu\text{M h}$, ($C_{\text{av,ss}}$ > 7 μM) and/or C_{max} above 16 μM [29]. However, an even more profound antitumor benefit was observed at higher doses (250 mg/kg dose bid), which resulted in daily exposure of 700 $\mu\text{M h}$ ($C_{\text{av,ss}}$ of ~29 μM) and C_{max} ~ 50 μM [29].

Indoximod, has been tested in human cancer clinical trials in combination with different chemotherapeutic and immunotherapeutic agents, such as docetaxel, paclitaxel, gemcitabine, nab-paclitaxel, temozolomide, idaurubicin, daunorubicin, cytarabine, ipilimumab, pembrolizumab, nivolumab, sipuleucel-T, and vaccines in numerous clinical protocol (IND078189, IND120813, IND127155,

IND135600, IND016400). Available pharmacokinetic (PK) data obtained after dosing indoximod FB capsules or indoximod HCl tablets shows that indoximod has a linear and dose proportional PK profile at doses of up to 1200 mg/dose, with average maximum plasma concentration (C_{max}) of 13.7 μM and drug exposure (AUC_{∞}) of 114 $\mu\text{M h/dose}$, with inter dose exposure values $\text{AUC}_{0-12\text{h}}$ of 83 $\mu\text{M h/dose}$, which under a 1200 mg bid dosing schedule result in an average daily exposure value at steady state $\text{AUC}_{0-24\text{h,ss}}$ of 240 $\mu\text{M h}$. Increasing doses above 1200 mg/dose up to 2400 mg/dose results in a non-linear and less than dose proportional increase in exposure, reaching C_{max} values of 22 μM and AUC_{∞} of 170 $\mu\text{M h/dose}$ at 2400 mg [30,31] (and unpublished results). The pH-dependent solubility profile of indoximod (>20 mg/mL at pH 1 and < 2 mg/mL at pH 7.4), as well as the low permeability profile in Caco-2 assays suggests that the non-linear PK profile of indoximod is due to limiting intestinal permeability and absorption.

We hypothesized that increasing oral bioavailability and exposure of indoximod in humans would increase the fraction of patients that respond favorably to the treatment by expanding the pharmacodynamic effects to those mechanisms requiring higher concentrations of indoximod as well as by minimizing the inter-subject variability in exposure observed while dosing indoximod. However, the non-linear pharmacokinetic profile of this drug makes it unlikely that this could be solved by increasing the dose given to patients. For the above-mentioned reasons, we investigated whether indoximod prodrugs in different salt forms would increase solubility and absorption rate or reduce blood clearance to levels that increase the maximum concentration and exposure of indoximod. Moreover, we looked for prodrugs and their salts that could result in increased exposure when dosed orally and in pill (capsule or tablet) dosage formulation. The results of these investigations showed that selected prodrugs resulted in exposure increase upon oral administration.

2. Results and discussion

2.1. Compound design

Incorporating amino acids as an ester or amide to the parent drug is a known approach to improve the oral bioavailability of poorly absorbed compounds [32–40]. Various transporters expressed in the intestinal epithelial cells can be targeted via amino acid derivatives to promote absorption of the amino acid based prodrugs [41–46]. In the case of indoximod, which is an *N*-methylated derivative of *D*-tryptophan, incorporating the amino acid is possible via both the amino and carboxyl groups. Therefore, we explored the formation of dipeptides with indoximod by conjugation of an amino acid to the amino or carboxyl group of indoximod, with the purpose to facilitate absorption of amino acids through the amino acid transporter LAT1 and LAT2 or peptide transporters PEPT1 and PEPT2 present in the intestinal epithelial cells [47–51]. Given that indoximod is required at relatively high daily doses (>2 g/day), we explored prodrugs of indoximod that were metabolized into molecules with a well-known and good safety profile, such as other α -amino acids, or alcohols such as glycerol and ethanol, as well as other moieties. These molecules were conjugated with indoximod as esters or amide groups at the carboxyl terminus to increase their LogP, thus potentially enhancing passive absorption through the intestinal membrane [52–54]. Additionally, we tested whether carbamates would improve absorption by eliminating the ionization of amino group under physiological conditions [53]. We synthesized the following classes of prodrugs: 1) esters of indoximod, derived from ethanol (**2-Cl**), isopropanol (**3-Cl**), benzyl alcohol (**6-Cl**), glycerol (**8-Cl**), L-Ser (**10-Cl**), piperidin-4-ylmethanol (**12-Cl**), 2-(piperidin-4-yl)ethan-1-ol (**14-Cl**), 2-

(dimethylamino)ethan-1-ol (**16-CI**), 2-(tetrahydro-2H-pyran-4-yl)ethan-1-ol (**18-CI**); 2) Indoximod-C(O)NHR, where the C terminal group forming an amide bond with indoximod is L-Val (**20-CI**); 3) carbamates **21** and **22**; 4) *N*-AA-indoximod; dipeptides of indoximod where the N-terminal amino acid is a natural L-amino acid (AA) such as Gly (**25-CI**), L-Ala (**28-CI**), L-Val (**31-CI**), L-Glu (**34-CI**), L-Gln (**37-CI**), L-Ile (**40-CI**), L-Leu (**43-CI**), L-Lys (**46-CI**), L-Phe (**49-CI**), L-Trp (**52-CI**); 5) *N*-NNAA-indoximod; dipeptides where the N-terminal amino acid is a non-natural amino acid (NNAA) such as D-Trp (**55-CI**) or indoximod (**58-CI**); and 6) *N*-AA-indoximod-COOEt; dipeptides of indoximod where the C-terminus of indoximod is an acetylated ester, and the N-terminal amino acid is a natural L-amino acid, such as L-Gln (**59-CI**), L-Ile (**60-CI**), L-Phe (**61-CI**), L-Leu (**62-CI**), L-Met (**64-CI**).

2.2. Chemistry

Ethyl **2-CI** and isopropyl **3-CI** esters of indoximod were synthesized by the thionyl chloride assisted esterification with ethyl and isopropyl alcohol, respectively.

Benzyl ester **6-CI** was synthesized via three step sequence involving Boc protection of free amine, esterification with benzyl bromide followed by Boc deprotection using hydrochloric acid in ethyl acetate. Compounds **10-CI**, **12-CI**, **14-CI**, **16-CI**, **18-CI** and **20-CI** were synthesized from Boc protected indoximod via a two-step sequence involving HATU ester and amide coupling and Boc deprotection using HCl or HCl/TFA. The deprotection of diol and Boc deprotection in **7** was carried with a mixture of TFA/H₂O/HCl in THF to afford **8-CI**. Ethyl (**21**) and neopentyl (**22**) carbamates were prepared by allowing indoximod to react with the corresponding chloroformates in the presence of NaHCO₃ (Scheme 1).

HATU coupling of ethyl (**2-CI**) and benzyl (**6-CI**) esters of indoximod with several natural and non-natural amino acids afforded the intermediates **23**, **26**, **29**, **32**, **35**, **38**, **41**, **44**, **47**, **50**, **53**, **56**, and **63**. The ester functionality was removed by hydrolysis to generate the corresponding acid derivatives. Boc deprotection of amides (**24**, **27**, **30**, **33**, **35**, **36**, **38**, **39**, **41**, **42**, **45**, **47**, **48**, **51**, **54**, **57** and **63**) was achieved with HCl in dioxane to yield the hydrochloride salts **25-CI**, **28-CI**, **31-CI**, **34-CI**, **59-CI**, **37-CI**, **60-CI**, **40-CI**, **62-CI**, **43-CI**, **46-CI**, **61-CI**, **49-CI**, **52-CI**, **55-CI**, **58-CI** and **64-CI**, respectively (Scheme 2).

The hydrochloric salt of prodrugs **8-CI**, **12-CI**, **59-CI**, **62-CI**, and **64-CI** were neutralized with aqueous sodium bicarbonate to yield the corresponding free base forms; **25-CI** and **46-CI** were run through an ion exchange chromatographic column to obtain the corresponding free base form. The free bases were subsequently converted to the monophosphate (**8-P**, **12-P**, **25-P**, **46-P**, **59-P**, **62-P**, and **64-P**), mesylate (**8-M**, **59-M**, and **62-M**), besylate (**62-B**) and bisulfate (**8-S**, **46-S**, **59-S**, and **62-S**) salts with phosphoric, methanesulfonic, benzene sulphonic and sulfuric acids in ethanol, respectively (Scheme 3).

The selected prodrug, **62-CI** (also known as development compound **NLG802**) was crystallized from ethanol/ethylacetate for single crystal X-ray data (Fig. 1).

2.3. Biological evaluation

2.3.1. In vitro stability in biological matrices

The different prodrugs were evaluated by several in vitro and in vivo criteria. First, we tested the stability of the prodrugs in buffered solutions at pH1 and pH7.4, as well as in simulated gastric fluid (SGF) and simulated intestinal fluid (SIF). Ideally, the prodrugs should be sufficiently stable through the acidic conditions of the stomach and neutral pH conditions of the small intestine and be transformed to the desired metabolite after intestinal absorption

and distribution through systemic circulation. For these reasons, we tested the chemical stability of the prodrugs (5 μM) after incubation in buffered pH1 and SGF solutions for 1.5 h, an average gastric residence time under fed conditions, and after a 6 h incubation at pH 7.4 and SIF, to simulate stability through the small intestine transit. Since these prodrugs were intended to be orally dosed to animals in solution, we tested that they were chemically stable in saline solution as a generic dosing vehicle. Additionally, we tested the stability after a 2 h incubation in mouse and rat plasma, and after a 6 h and 24 h incubation in human plasma, where we expected to see moderate to high conversion of the prodrugs into indoximod. Table 1 shows the percentage of prodrug remaining after incubation at 37 °C, in the corresponding solvent for the indicated period, relative to a sample incubated in the same vehicle for 0 min, immediately extracted with acetonitrile and stored at -80 °C until analysis. Each prodrug was quantified using a specific LC-MS/MS analytical method developed for each test compound.

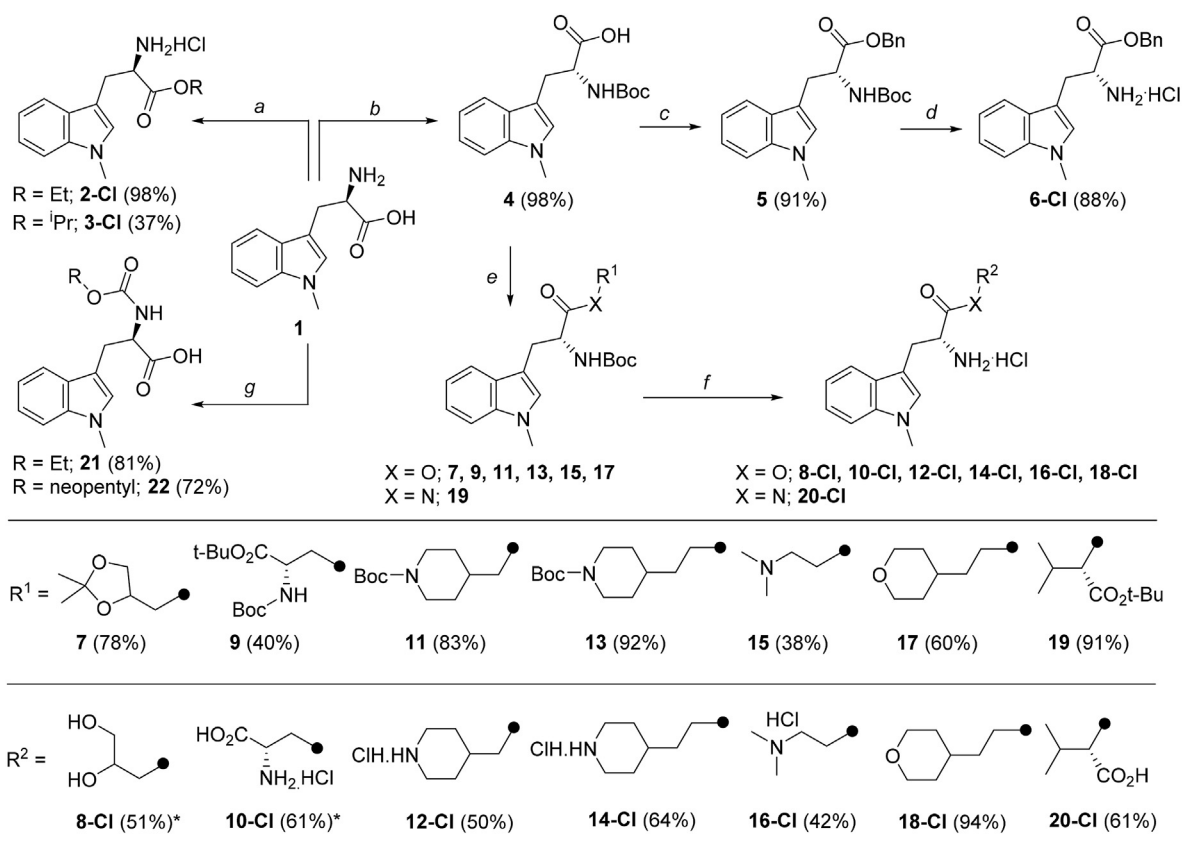
At pH1 most of the prodrugs were stable (≥50%) after 1.5 h, with the exception of **8-CI**, **12-CI** and **58-CI**, which were moderately stable (20–50%), and **10-CI** and **16-CI** which were found to be highly unstable (<20%). Curiously, **10-CI** was more stable in SGF than in buffer at pH 1, and **28-CI** was unstable despite being very stable in buffer at pH 1 suggesting that it might be sensitive to pepsin mediated cleavage.

At neutral pH7 most of the prodrugs were stable (≥50%) except for **10-CI** and **16-CI**, which were hydrolyzed completely after 6 h. In SIF most prodrugs were stable except for **8-CI**, **12-CI**, and **28-CI**, which were moderately stable and **10-CI** and **16-CI** which were completely unstable. Compounds **12-CI**, **14-CI**, **16-CI** and **28-CI** showed to be somewhat unstable after 24 h incubation in dosing vehicle formulation. A higher stability for most of the tested prodrugs at pH 1 or 7 and in SGF and SIF indicates that the prodrugs can easily pass through the stomach with minor degradation and once absorbed can be easily hydrolyzed by liver and plasma to release indoximod.

The results in plasma varied among plasma species and class of compounds. In general, compounds of Class 4 and Class 5 (dipeptides with natural or non-natural amino acids with no ester protecting groups on the C-terminus) were stable in plasma of all three species, with the exception of **31-CI** and **49-CI** which were more unstable in rat plasma. Generally, compounds of Class 1 and compounds of Class 6 (esters of indoximod) were very unstable in rodent plasma and more stable human plasma even after longer incubation periods suggesting differences in substrate preferences for esterases present in rodent vs human plasma. Of note, **8-CI**, **10-CI**, **12-CI**, **14-CI**, **16-CI**, **59-CI** and **62-CI**, showed moderate conversion in human plasma, though only **14-CI**, **59-CI**, and **62-CI** satisfy the criteria of being stable in gastric and intestinal simulated conditions. These results suggested that these compounds can pass through the stomach with slow degradation and the absorbed molecules from the gastrointestinal tract can be rapidly converted into the active form in plasma. Compounds of Class 2 (C-terminal dipeptides) and Class 3 (carbamates), showed to be very stable in plasma from all 3 species. Since prodrug conversion can take place in the liver as well as in systemic circulation, the stability in plasma was informative, but was not used a criterion to discard prodrugs that were stable in plasma from further in vivo testing.

2.3.2. Pharmacokinetic testing of indoximod prodrugs in liquid formulation in rats

A preliminary assessment of the pharmacokinetic profile of a few prodrugs was carried out in rats dosed with the prodrug in liquid formulation. Indoximod or its prodrugs were dosed to rats by oral gavage at 50 mg/kg, blood samples were collected at 0, 0.5, 1, 2,



Scheme 1. Synthesis of **2-Cl**, **3-Cl**, **6-Cl**, **8-Cl**, **10-Cl**, **12-Cl**, **14-Cl**, **16-Cl**, **18-Cl**, **20-Cl**, **21** and **22**. Reagents and conditions: a) ROH, SOCl₂, 80 °C, 17 h; b) NaOH, Boc₂O, dioxane, 0 - rt, 16 h, 98%; c) BnBr, Cs₂CO₃, DMF, rt, 2 h, 91%; d) HCl, EtOAc, 0 °C - rt, 2.75 h, 88%; e) R¹OH or R²NH₂, HATU, DIPEA, CH₃CN, 0 °C to rt, 17 h, 38–92%; f) HCl (4 M in dioxane), dioxane, rt, 2.5 h, 42–94%; g) i) ClCO₂R, NaHCO₃, THF, 0.5 h; ii) HCl, 0 °C. *a mixture of TFA and HCl was used.

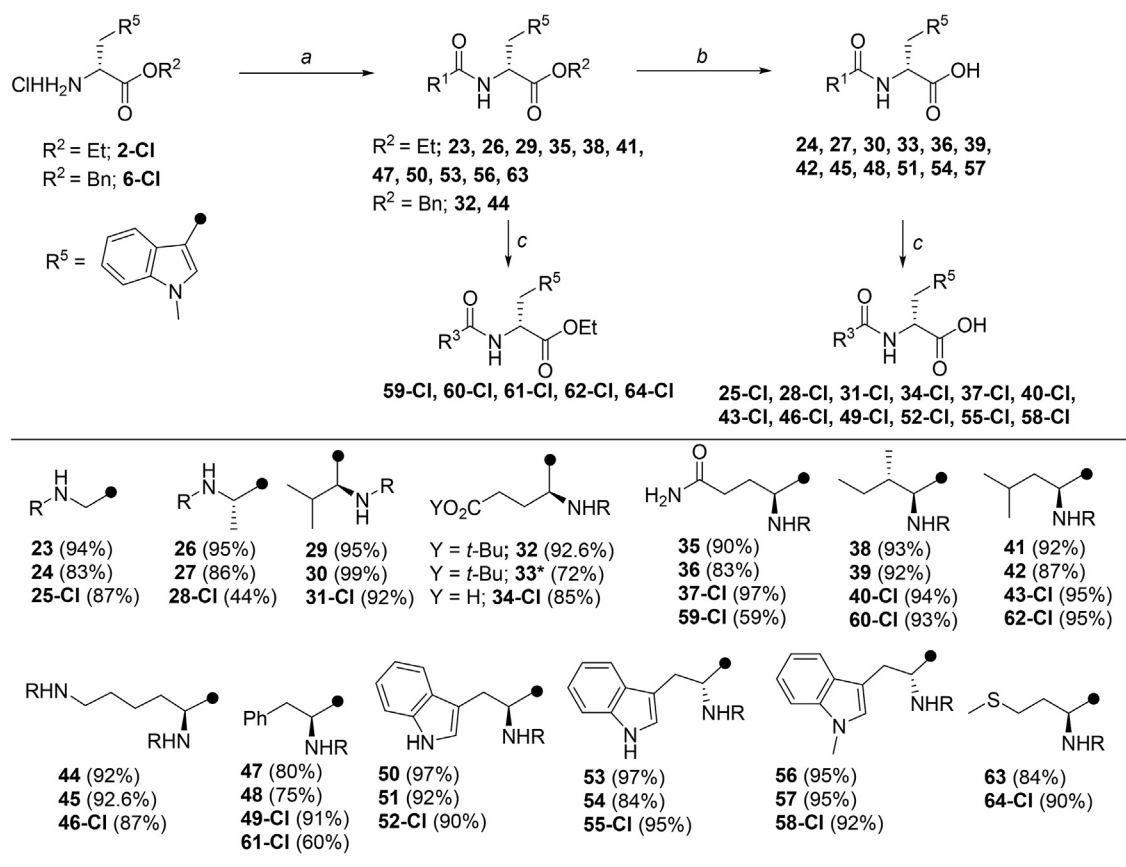
4, 10, 24, 48 and 72 h, plasma concentration of indoximod was determined by LC-MS/MS, and pharmacokinetic parameters for indoximod calculated using non-compartmental analysis. Since all rats were orally dosed at 50 mg/kg, but each prodrug has different molecular weight, in order to compare the values of maximum peak concentration (C_{max}) and total area under the curve (AUC_{∞}) obtained after dosing each prodrug vs. those obtained after dosing indoximod, the measured C_{max} and AUC_{∞} values were normalized by multiplying them by the ratio of $MW_{Prodrug}/MW_{Indoximod}$, thus assuming linear pharmacokinetics within an approximately 2-fold dose range. Table 2 shows that the ethyl ester of indoximod (**2-Cl**) produced a relative increase in both C_{max} and AUC_{∞} compared to dosing indoximod, which is consistent with this prodrug being stable in simulated gastric and intestinal fluids and very labile in rat plasma. However, the similar prodrugs isopropyl ester **3-Cl** and benzyl ester **6-Cl** showed a moderate decrease in exposure, while carbamate prodrugs **21** and **22** showed a marked decrease in exposure parameters and were not characterized any further. No apparent correlation was observed between changes in exposure parameters and increase in $cLogP$ in this reduced set of prodrugs.

A caveat of the comparison between dosing prodrugs vs indoximod as a free base was that prodrugs were fully soluble in the dosing formulation, while indoximod was insoluble at doses of 50 mg/kg. This may result in a time-dependent controlled release effect for indoximod which could result in lower C_{max} but higher AUC_{∞} than when dosed in fully soluble form. Therefore, for further comparisons and to ensure full dissolution of indoximod and each prodrug appropriate vehicles were used (saline solution, Cremaphor®: EtOH: saline (10:10:80), or Chremaphor: EtOH: saline: HCl

(10:10:80:0.1 N)) and the dose was reduced to 10 mg/kg. The use of solution formulation ensured that only the differences in intestinal permeability and in vivo conversion of prodrugs to indoximod would be assessed by characterization of the PK parameters, excluding the effects of differences in solubility or solubilization rate of different prodrugs, different salt forms and polymorphs, which could indirectly impact the observed absorption rate.

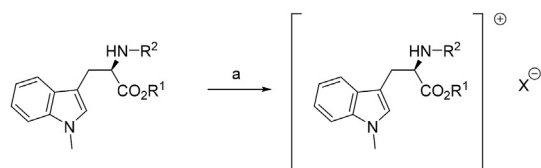
Table 3 shows the relative change in indoximod C_{max} and AUC_{∞} and their normalized values after orally dosing each one of the test prodrugs in solution at 10 mg/kg. In general, there did not seem to be a correlation between the class or prodrug or their $cLogP$ and the change in the normalized values of C_{max} and/or AUC_{∞} . Generally, prodrugs from classes 1, 4, or 6 produced an increase in AUC_{∞} , though some prodrugs from those classes also resulted in relative decreases in AUC_{∞} , suggesting that a combination of factors might be affecting the performance of each prodrug.

Table 3 shows that some prodrugs resulted in an effective increase in either C_{max} , AUC_{∞} or both pharmacokinetic parameters. In particular, exposure (AUC_{∞}) to indoximod seems to be enhanced when dosing **12-Cl**, **62-Cl**, **59-Cl**, **46-Cl**, **18-Cl**, **16-Cl**, **43-Cl**, **60-Cl**, **25-Cl**, **8-Cl**, **10-Cl**, and **34-Cl**, while indoximod C_{max} seems to be enhanced when dosing **16-Cl**, **8-Cl**, **25-Cl**, **59-Cl**, **43-Cl**, **2-Cl** and **12-Cl**. **2-Cl** resulted in a 11% reduction in AUC when dosed at 10 mg/kg but in a 126% increase in AUC at 50 mg/kg, possibly due to saturation of elimination mechanisms after absorption. Since the prodrugs were administered in completely soluble form, this suggests that those prodrugs that show enhanced exposure of indoximod in plasma do so by a mechanism that involves a combination of factors including enhanced permeability of the prodrug through the



R¹ is substituent with Boc; **R** = Boc for **23**, **24**, **26**, **27**, **29**, **30**, **32**, **33**, **35**, **36**, **38**, **39**, **41**, **42**, **44**, **45**, **47**, **48**, **50**, **51**, **53**, **54**, **56**, **57** and **63**. **R³** is substituent without Boc; **R** = H·HCl for **25-Cl**, **28-Cl**, **31-Cl**, **34-Cl**, **37-Cl**, **40-Cl**, **43-Cl**, **46-Cl**, **49-Cl**, **52-Cl**, **55-Cl**, **58-Cl**, **59-Cl**, **60-Cl**, **61-Cl**, **62-Cl** and **64-Cl**.

Scheme 2. HATU coupling and ester hydrolysis of indoximod prodrug intermediates. Reagents and conditions: a) **R¹CO₂H**, HATU, DIPEA, CH₃CN, 0 °C-rt, 17 h, 71–97%; b) i) LiOH·H₂O, THF, H₂O, rt, 2 h; *for **33** NaOH, MeOH, THF, 0 °C, 1 h; ii) 1 M HCl, 40–99%; c) HCl (4 M dioxane), 0 °C - rt, 2.5–18 h.



Scheme 3. Synthesis of different salts from the free base form of **8-Cl**, **12-Cl**, **25-Cl**, **46-Cl**, **59-Cl**, **62-Cl** and **64-Cl**. Reagents and conditions: a) **X** = H₃PO₄, or CH₃SO₃H, or PhSO₃H, or H₂SO₄, EtOH, 0 °C to rt, 5–18 h.

intestinal cell wall, reduced clearance of the prodrug with respect to indoximod and good rate of hydrolysis of the prodrug to indoximod *in vivo*.

2.3.3. Pharmacokinetic testing of indoximod prodrug salts in solid capsule formulation in rats

To test which prodrugs have the best combined set of pharmacological properties (solubilization rate, solubility, intestinal permeability, clearance rate and rate of metabolism to indoximod) that would result in increased exposure to indoximod after oral dosing in a capsule formulation, the prodrugs that showed enhanced indoximod C_{max} or AUC_∞ when dosed in solution were prepared in different salt forms and mixed with excipients to form a powder blend. These blends were formulated in capsules containing the same molar dose of each prodrug. Gelatin capsules were

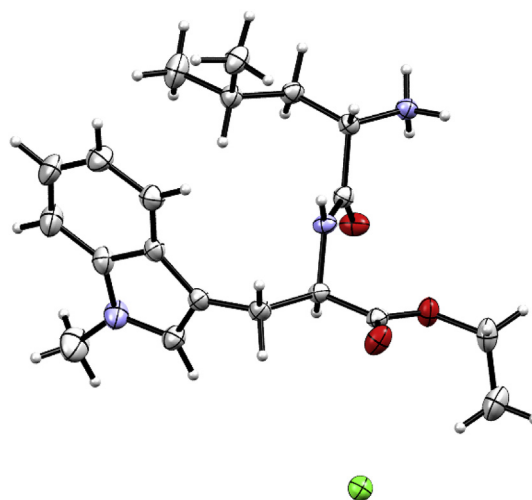


Fig. 1. Single crystal X-ray of NLG802.

prepared containing 11, 28 or 50 μmol of indoximod or each prodrug per capsule (Supplementary Information, Table 1). One to three capsules were administered to rats by intra stomach delivery at target doses of 37, 185 or 500 μmol/kg, equivalent to indoximod

Table 1
Chemical stability of indoximod prodrugs.^a

Compound	Class	Saline	Buffer				Simulated Fluids				Plasma				
			pH 1		pH 7.4		SGF		SIF		Mouse	Rat	Human		
			24 h	1.5 h	24 h	6 h	24 h	1.5 h	24 h	3 h	24 h	2 h	2 h	6 h	24 h
2-Cl	1	100	59	100	94	52	83	85	64	0	0	0	0	93	35
3-Cl	1	ND	ND	ND	ND	ND	ND	ND	ND	ND	0	0	0	ND	ND
8-Cl	1	99	37	99	50	29	62	58	34	10	0	0	0	33	11
6-Cl	1	ND	ND	ND	ND	ND	ND	ND	ND	ND	0	0	0	ND	ND
10-Cl	1	70	10	70	0	0	56	56	0	0	80	84	0	0	0
12-Cl	1	23	36	23	92	12	75	73	45	3	0	19	44	2	2
14-Cl	1	46	74	46	91	22	90	90	62	8	0	0	0	27	4
16-Cl	1	47	3	47	0	0	2	2	0	0	0	0	0	10	2
18-Cl	1	76	52	76	85	0	85	60	67	0	0	0	0	85	54
20-Cl	2	98	51	98	99	37	54	49	62	64	89	100	68	39	39
21	3	ND	ND	ND	ND	ND	ND	ND	ND	ND	97	100	ND	ND	ND
22	3	ND	ND	ND	ND	ND	ND	ND	ND	ND	100	100	ND	ND	ND
25-Cl	4	99	64	99	83	65	80	78	64	38	100	56	78	68	68
28-Cl	4	40	100	40	58	34	20	25	36	12	94	92	65	0	0
31-Cl	4	99	98	99	91	44	55	50	78	76	57	9	79	47	47
34-Cl	4	91	99	91	81	60	90	88	88	85	100	100	90	86	86
37-Cl	4	78	65	78	100	74	83	83	53	0	49	100	93	83	83
40-Cl	4	98	92	98	100	100	81	77	94	0	80	54	84	86	86
43-Cl	4	99	92	99	95	95	95	97	66	0	88	100	87	82	82
46-Cl	4	100	89	100	93	57	97	92	96	96	77	95	96	78	78
49-Cl	4	92	96	92	89	92	79	80	91	0	66	19	87	75	75
52-Cl	4	61	52	61	55	33	81	73	88	69	90	76	97	94	94
55-Cl	5	87	53	87	81	45	51	48	53	51	82	79	77	32	32
58-Cl	5	91	45	91	100	34	63	49	81	77	65	80	92	82	82
59-Cl	6	85	73	85	67	17	108	88	70	1	0	0	23	0	0
60-Cl	6	97	95	97	97	63	98	97	91	38	0	0	75	16	16
61-Cl	6	90	99	90	96	96	89	86	65	0	0	0	68	11	11
62-Cl	6	87	90	87	92	48	92	88	91	30	0	0	53	6	6

a: % remaining reported. ND: not determined. Mur: murine.

Table 2
Change in C_{max} and AUC for Indoximod after Orally Dosing Rats with Solutions of Indoximod or its Prodrugs at a dose of 50 mg/kg.

Drug/Prodrug	Salt	MW g/mol	Dose mg/kg	n	C_{max}	Dose Norm. C_{max}	% Change in Norm. C_{max}	AUC_{∞}	Dose Norm. AUC_{∞}	% Change in Norm AUC_{∞}	cLogP
					μM	μM	%	μMh	μMh	%	
Indoximod	HCl	218	50	1	27	27	0%	1323	1323	0%	-1.10
2-Cl	HCl	246	50	1	58	66	143%	2645	2988	126%	1.96
3-Cl	FB	261	50	1	23.4	28	4%	877	1051	-21%	2.27
6-Cl	HCl	345	50	1	17.8	28	4%	650	1028	-22%	3.14
21	FB	290	50	1	4.5	6.0	-78%	172	229	-83%	2.34
22	FB	333	50	1	0.10	0.15	-99%	3.6	5.5	-100%	3.66

n: number of rats; C_{max} (μM): maximum concentration of indoximod observed in plasma. Value is the average of n values.

Norm. C_{max} (μM): C_{max} normalized to the same molar dose ($\mu mol/kg$) obtained by multiplying the observed C_{max} of indoximod in plasma by $MW_{prodrug}/MW_{indoximod}$ **% Change in Norm. C_{max}** : Calculated as $[C_{max}(\text{indoximod from Prodrug})/C_{max}(\text{indoximod from indoximod}) - 1] \times 100$; **AUC_{∞} ($\mu M.h$)**: Area under the curve [indoximod] vs Time observed in plasma. Value is the average of n values; **Norm. AUC_{∞} ($\mu M.h$)**: Average AUC_{∞} normalized to the same molar dose ($\mu mol/kg$); obtained by multiplying the observed average AUC_{∞} of indoximod in plasma by $MW_{prodrug}/MW_{indoximod}$; **% Change in AUC_{∞}** : calculated as $[AUC_{\infty}(\text{indoximod from prodrug})/AUC_{\infty}(\text{indoximod from indoximod}) - 1] \times 100$.

dosing at 8, 40 and 110 mg/kg, respectively (See methods).

Table 4 shows that **12-Cl** or **12-P** resulted in a significant decrease in C_{max} (69–79%, $p < 0.004$) and AUC_{∞} (54–64%, $p < 0.014$) for indoximod. Since this compound showed an increase in C_{max} (24%) and AUC_{∞} (75%) when administered via oral solution, the difference in solubilization rate or final solubility may account for the observed differences when administered in powder form. Other prodrugs such as **59**, **59-Cl**, **59-P**, **59-M**, **25-Cl**, **25-P**, **46**, **46-Cl**, **46-S** or **46-P** produced minor and non-statistically significant variations in the C_{max} or AUC_{∞} for indoximod compared to an equivalent molar dose of indoximod.

The glycerol ester **8-P** produced a significant increase in C_{max} (37–153%) and AUC_{∞} (21–75%) at doses of up to 185 $\mu mol/kg$, while **8-Cl**, **8-S** and **8-M** resulted in no significant changes in indoximod exposure.

A new methionyl derivative prodrug **64-Cl** introduced at this stage of development showed a significant increase in C_{max}

(59–152%) and AUC_{∞} (49–76%) at doses $\geq 185 \mu mol/kg$ in its hydrochloride or phosphate salt forms.

The L-leucyl prodrug **62** in its hydrochloride (**62-Cl**), phosphate (**62-P**), mesylate (**62-M**) or besylate (**62-B**) salt forms dosed at 37–185 $\mu mol/kg$ was able to significantly increase AUC_{∞} of indoximod by 33–127%, while its sulfate salt (**62-S**) did not result in a significant increase in C_{max} or AUC_{∞} at equivalent doses. Similarly, significant increases in C_{max} were observed for **62-Cl**, **62-P** or **62-M** salts. At doses of 500 $\mu mol/kg$, **62-Cl**, showed a minor increase in C_{max} and AUC_{∞} compared to indoximod indicating a possible saturation of absorption or prodrug conversion at these high dose levels.

2.3.4. Pharmacokinetic testing of indoximod prodrug salts in solid capsule formulation in Cynomolgus monkeys

Since the rat shows a non-saturable linear increase in exposure with doses of indoximod of up to 100 mg/kg, while humans show a

Table 3
Change in C_{max} or AUC_{∞} for Indoximod after Orally Dosing Rats with Solutions of Indoximod or its Prodrugs.

Prodrug ID	Class	Salt form	MW	Dose	n	C_{max}	Norm. C_{max}	% Change in Norm. C_{max}	AUC_{∞}	Norm. AUC_{∞}	% Change in Norm AUC_{∞}	cLogP
			g/mol	mg/kg		μM	μM	%	$\mu M \cdot h$	$\mu M \cdot h$	%	
Indoximod		HCl	218	10	5	17.3	17.3	0	508	508	0	-1.10
12-Cl	1	HCl	389	10	5	12.1	21.5	24	500	889	75	1.66
62-Cl	6	HCl	396	10	3	9.3	16.2	-6	490	888	75	3.16
59-Cl	6	HCl	411	10	5	13	24.4	41	428	806	58	-0.11
46-Cl	4	HCl	419	10	5	8.7	16.7	-3	414	795	56	-0.04
18-Cl	1	HCl	367	10	3	8.9	15	-14	460	774	52	2.21
16-Cl	1	HCl	362	10	3	23.8	39.5	128	440	731	44	1.75
43-Cl	4	HCl	368	10	3	14.5	24.4	41	366	617	21	0.24
60-Cl	6	HCl	396	10	3	7.1	12.8	-26	334	606	19	3.16
25-Cl	4	HCl	312	10	3	19.6	28	62	419	599	18	-1.52
8-Cl	1	HCl	329	10	5	22.1	33.3	92	395	595	17	-0.04
10-Cl	1	HCl	378	10	3	7.7	13.3	-23	339	588	16	-1.16
34-Cl	4	HCl	384	10	3	10	17.6	2	326	574	13	-2.10
2-Cl	1	HCl	283	10	3	17	22	27	350	454	-11	1.96
49-Cl	4	HCl	402	10	3	6.4	11.9	-31	231	425	-16	0.20
52-Cl	4	HCl	368	10	3	7.1	12	-31	246	415	-18	0.19
37-Cl	4	HCl	383	10	3	4.8	8.5	-51	212	372	-27	-3.02
31-Cl	4	HCl	354	10	3	8.8	14.2	-18	209	338	-33	0.28
61-Cl	6	HCl	430	10	3	4	7.9	-54	167	329	-35	3.12
40-Cl	4	HCl	368	10	3	7.4	12.5	-28	187	316	-38	0.24
28-Cl	4	HCl	326	10	3	9	13.4	-22	207	310	-39	-1.21
58-Cl	5	HCl	455	10	3	1.5	3	-83	126	262	-48	0.66
20-Cl	2	HCl	354	10	3	1	1.6	-91	125	202	-60	-0.28
55-Cl	5	HCl	441	10	3	1.6	3.2	-82	90	182	-64	2.19
14-Cl	1	HCl	402	10	3	1.3	2.4	-86	59.9	110	-78	2.19

n: number of rats; C_{max} (μM): maximum concentration of indoximod observed in plasma. Value is the average of n values.

Norm. C_{max} (μM): C_{max} normalized to the same molar dose ($\mu mol/kg$) obtained by multiplying the observed C_{max} of indoximod in plasma by $MW_{prodrug}/MW_{indoximod}$. % Change in Norm. C_{max} : Calculated as $[C_{max}(\text{indoximod from Prodrug})/C_{max}(\text{indoximod from indoximod}) - 1] \times 100$; AUC_{∞} ($\mu M \cdot h$): Area under the curve [indoximod] vs Time observed in plasma. Value is the average of n values; Norm. AUC_{∞} ($\mu M \cdot h$): Average AUC_{∞} normalized to the same molar dose ($\mu mol/kg$); obtained by multiplying the observed average AUC_{∞} of indoximod in plasma by $MW_{prodrug}/MW_{indoximod}$; % Change in AUC_{∞} : calculated as $[AUC_{\infty}(\text{indoximod from prodrug})/AUC_{\infty}(\text{indoximod from indoximod}) - 1] \times 100$.

saturable exposure above doses of 10 mg/kg [30,31], we tested in primates two of the prodrugs that showed the largest increase in AUC_{∞} to investigate whether the monkey could be a better model to predict human pharmacokinetics for indoximod than rats. Cynomolgus monkeys were dosed with indoximod, **62-Cl** or **64-Cl** at doses of 92, 275 or 875 $\mu mol/kg$ in a crossover study design where each animal received the same single molar dose of either indoximod, **62-Cl** or **64-Cl** every 7 days. These prodrugs were mixed with excipients and formulated into capsules of different dose strengths (Suppl. Materials, Table 2). Animals were orally dosed with 1 or 3 capsules A (458 $\mu mol/capsule$) or 4 capsules B (1032 $\mu mol/capsule$). Blood samples were collected at 0, 5 min, 15 min, 30 min, 1, 2, 4, 8, 12, 24, 26 and 48 h post-dose, the concentrations of prodrug and indoximod were analyzed by validated LC-MS/MS methods and PK parameters were calculated by non-parametric methods.

Table 5 shows that both **62-Cl** and **64-Cl** significantly increase parameters of exposure for indoximod, with **62-Cl** showing slightly higher increases in AUC_{∞} than equivalent molar doses of **64-Cl** and **64-Cl** showing higher C_{max} values at the highest dose level. A comparison of the dose dependent exposure parameters for indoximod (C_{max} and AUC_{last}) after orally dosing indoximod capsules with similar excipient compositions at allometrically comparable doses to either monkeys or humans shows that monkeys are a good model to predict the dose-dependent exposure of indoximod (Fig. 2), both in the values of C_{max} and AUC and with comparable dose-dependent saturation profile. Administration of these prodrugs to monkeys produced a larger and significant increase in indoximod exposure in monkeys (~4-5-fold) compared to rats, suggesting that a significant improvement in indoximod exposure could be expected in humans after administration of **62-Cl** or **64-Cl**.

2.3.5. Selection of clinical candidate

Of all the tested prodrugs, **62-Cl** was selected as the development candidate. First, it was stable in simulated gastric and intestinal fluids, and demonstrated a good conversion in human plasma. Second, it produced increased exposure when dosed to rats in solution and in capsule form, and most importantly, it resulted in increased exposure of indoximod when dosed in capsule form to non-human primates. Among other salts of **62-Cl**, only the mesylate salt showed better increase in exposure than the hydrochloride salt when dosed to rats in capsule form. However, the mesylate had disadvantages for pharmaceutical development, such as higher molecular weight, hygroscopicity, and the need to implement strict controls to avoid the formation of genotoxic impurity ethyl methane sulfonate. Since the estimated daily dose of these prodrugs in humans is in the range of 1.2–2.4 g/dose, trying to minimize the molecular weight is important to reduce the drug load per tablet capsule form. Additionally, a daily dose of more than 2 g requires strict controls in the levels of genotoxic impurities. Compared to **62-Cl**, **64-Cl** produced slightly smaller exposure values for C_{max} and AUC_{∞} at doses of up to 3300 $\mu mol/m^2$ in monkeys, has higher molecular weight, potential long-term stability concerns of the pharmaceutical preparation, and possible formation of undesired oxidation metabolites due to the presence of the methionine residue. For these reasons, **62-Cl** (**NLG802**) was selected as the preclinical development candidate.

2.4. Pharmacological characterization of NLG802

2.4.1. Characterization of NLG802 drug substance

NLG802 (**62-Cl**, MW 395.93 g/mol) is a crystalline white powder, with LogP 2.6, LogD^{7.4} of 2.3 and pKa of 7.76. It is not hygroscopic

Table 4
Comparison of C_{max} and total exposure (AUC_{∞}) between indoximod free base vs. its prodrugs in different salt forms after oral dosing of rats with capsules.

Drug/Prodrug	Salt form	Dose	n	C_{max}	% Change in C_{max}	p	AUC_{∞}	% Change in AUC_{∞}	p	
		$\mu\text{mol/kg}$		(μM)			($\mu\text{M}\cdot\text{h}$)			
Indoximod	Free base	37	11	15.9 ± 8	0		390 ± 166	0		
		185	8	20.8 ± 4	0		1080 ± 478	0		
		500	6	76.2 ± 25	0		2871 ± 1379	0		
12-Cl	HCl	37	4	4.9 ± 0.4	-69	0.008	180 ± 18	-54	0.014	
12-P	H ₃ PO ₄	37	4	3.3 ± 1	-79	0.004	141 ± 45	-64	0.006	
46	free base	37	4	13.3 ± 2	-17	0.26	340 ± 57	-13	0.28	
46-Cl	HCl	37	4	17.2 ± 9	8	0.39	350 ± 83	-10	0.33	
46-S	H ₂ SO ₄	37	4	15.3 ± 5	-4	0.44	446 ± 101	10	0.27	
46-P	H ₃ PO ₄	37	4	11.5 ± 4	4	0.15	325 ± 61	-17	0.23	
59	free base	37	4	16.7 ± 9	5	0.43	327 ± 12	-16	0.24	
59-Cl	HCl	37	4	17.8 ± 4	12	0.33	386 ± 89	-1	0.48	
59-P	H ₃ PO ₄	37	4	10.9 ± 3	-32	0.12	280 ± 21	-28	0.11	
59-S	H ₂ SO ₄	37	4	19 ± 8	20	0.25	314 ± 105	-20	0.21	
59-M	CH ₃ SO ₃ H	37	4	16.5 ± 6	4	0.45	342 ± 97	-12	0.3	
25-Cl	HCl	37	4	17.5 ± 2	10	0.35	394 ± 103	1	0.48	
25-P	H ₃ PO ₄	37	4	15.4 ± 5	-3	0.45	403 ± 153	3	0.45	
8-Cl	HCl	37	4	20.2 ± 5	28	0.16	472 ± 58	21	0.18	
8-P	H ₃ PO ₄	37	8	21.7 ± 3	37	0.032	571 ± 95	46	0.0067	
8-M	CH ₃ SO ₃ H	H ₃ PO ₄	185	7	52.8 ± 23	153	0.0002	1896 ± 765	75	0.014
		37	4	11.6 ± 5	-27	0.16	285 ± 39	-27	0.12	
8-S	H ₂ SO ₄	37	4	17.6 ± 2	2	0.34	472 ± 120	21	0.19	
64-P	H ₃ PO ₄	37	8	21.0 ± 11	32	0.13	400 ± 136	2	0.45	
		185	8	31.1 ± 8	49	0.003	1236 ± 498	14	0.27	
64-Cl	HCl	37	8	19.2 ± 6	21	0.16	439 ± 114	13	0.24	
		185	8	52.4 ± 15	152	<0.0001	1898 ± 852	76	0.017	
		500	6	121 ± 46	59	0.031	4269 ± 1255	49	0.048	
62-Cl	HCl	37	4	30.4 ± 10	92	0.005	664 ± 134	70	0.006	
		185	8	44.2 ± 10	112	<0.0001	1860 ± 609	87	<0.0001	
		500	6	80.0 ± 22	5	0.39	3300 ± 391	15	0.26	
62-P	H ₃ PO ₄	37	7	29.2 ± 13	84	0.008	628 ± 145	61	0.003	
		185	10	35.3 ± 7	69	0.0001	1433 ± 858	33	0.024	
62-M	CH ₃ SO ₃ H	37	4	33.6 ± 3	111	0.0004	886 ± 273	127	0.0004	
62-B	Besylate	37	4	20.5 ± 2	29	0.14	565 ± 82	45	0.034	
62-S	H ₂ SO ₄	37	4	12.2 ± 4	-23	0.19	369 ± 145	-5	0.41	

Table 5
Comparison of C_{max} and total exposure ($AUC_{0-\infty}$) between indoximod free base vs. NLG802 in different salt forms after oral dosing of Cynomolgus monkeys with capsules.

Drug/Prodrug ID	Salt form	Dose	n	C_{max}	% Change in C_{max}	p	AUC_{∞}	% Change in AUC_{∞}	p
		($\mu\text{mol/kg}$)		(μM)			($\mu\text{M}\cdot\text{h}$)		
Indoximod	free base	92	3	8.2 ± 0.4	0	—	38.5 ± 4	0	—
		275	3	17.5 ± 3	0	—	74.9 ± 5	0	—
		825	3	27.8 ± 8	0	—	165 ± 52	0	—
62-Cl	HCl	92	3	50.6 ± 8	518	0.0004	114 ± 2	195	<0.0001
		275	3	101 ± 28	476	0.003	463 ± 36	518	<0.0001
		825	2	92 ± 17	230	0.005	853 ± 349	416	0.017
64-Cl	HCl	92	3	33 ± 5	305	0.0005	90.7 ± 11	136	0.0007
		275	3	88 ± 32	402	0.009	370 ± 113	393	0.005
		825	3	142 ± 57	411	0.013	761 ± 516	369	0.059

(less than 0.08% weight gain in dynamic vapor sorption cycle from 0 to 80%RH) and soluble in water (19.8 mg/mL at 25 °C), SGF (17.1 mg/mL at 37 °C), FaSSIF (19.1 mg/mL, at 37 °C) as well as in buffered solutions ranging from pH 1.58–6.7 (16.3–21 mg/mL).

2.4.2. Metabolization of NLG802

Metabolite identification of **NLG802** was carried out after incubation for 2 h with primary hepatocytes from CD-1 mouse, Sprague Dawley rat, Beagle dogs, Cynomolgus monkey and human. A total of fifteen metabolites were detected by LC-UV-MSⁿ. **Table 6** and **Fig. 3** show the main metabolites, quantified by their %UV response. Metabolization profiles were very similar among rat, dog, monkey and human, with a few differences in the relative amounts of each metabolite formed. Mouse showed two additional metabolites. Overall, **NLG802** is extensively metabolized to indoximod via

hydrolysis to M9 which is further metabolized by hydrolysis to indoximod. Most species except human show a significant dehydrogenation to indoximod (M1). Since this metabolite is not formed after incubation of indoximod in primary hepatocytes from any species, it is likely that the M1 is formed by hydrolysis of M6/M7. In a carboxylesterase metabolism phenotyping study using recombinant CES enzymes expressed in insect cell Supersomes (CES1b, CES1c and CES2), formation of metabolite M9 was observed with CES1b and CES1c and not with CES2. Based on the sum of differences in percent of abundance for each metabolite with respect to that in humans, rat and monkey hepatocytes were the two species that showed a metabolite profile most similar to humans.

NLG802 showed moderate direct (IC_{50} 5 μM) and time-dependent (7-fold shift) inhibition of CYP3A4, weak inhibition to CYP2D6 (IC_{50} 19 μM) and CYP2C19 (IC_{50} 47 μM), no inhibition of

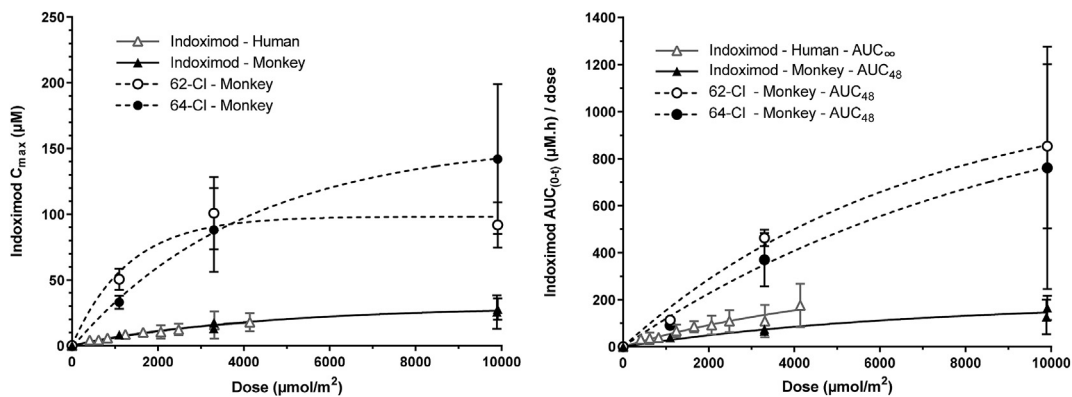


Fig. 2. Indoximod prodrugs 62-Cl and 64-Cl increase exposure to indoximod in monkeys.

Fig. 2. Comparison of C_{max} and AUC_{last} for indoximod after oral dosing of indoximod capsules of similar compositions to humans or monkeys, and after dosing capsules with indoximod prodrugs **62-Cl** and **64-Cl**. For better inter-species and inter-drug comparisons doses were allometrically scaled by surface area by multiplying the dose in mg/kg by 12 for monkeys or 37 for humans and then converted to μmoles . Human PK data was aggregated from several human clinical trials (NCI8045 [30,31], NCI8784, NLG2100 and NLG2102) after single oral dosing of indoximod free base capsules in the range of 200 mg–2000 mg, using 82 kg as the average patient weight for dose conversion.

Table 6

Metabolite identification in primary hepatocytes.

	Metabolite Relative Abundance (%UV area)												
	NLG802	M1	M2	M3	M4	M5	M6	M7	M8	M9	M10	M11	M12
Mouse	0.3	12.2	57.8	0.3	0.5	0.2	–	0.2	–	2.2	–	3.1	16.5
Rat	0.4	16.5	74.4	1.0	0.1	0.1	1.8	0.6	–	3.8	0.4	–	–
Dog	1.1	10.5	62.1	–	0.8	0.6	5.0	1.9	–	2.6	4.8	–	–
Monkey	1.3	11.9	70.7	0.5	1.3	1.3	2.6	0.4	1.3	7.6	1.0	–	–
Human	0.9	1.9	89	–	0.1	0.1	1.3	1.6	–	1.2	3.8	–	–

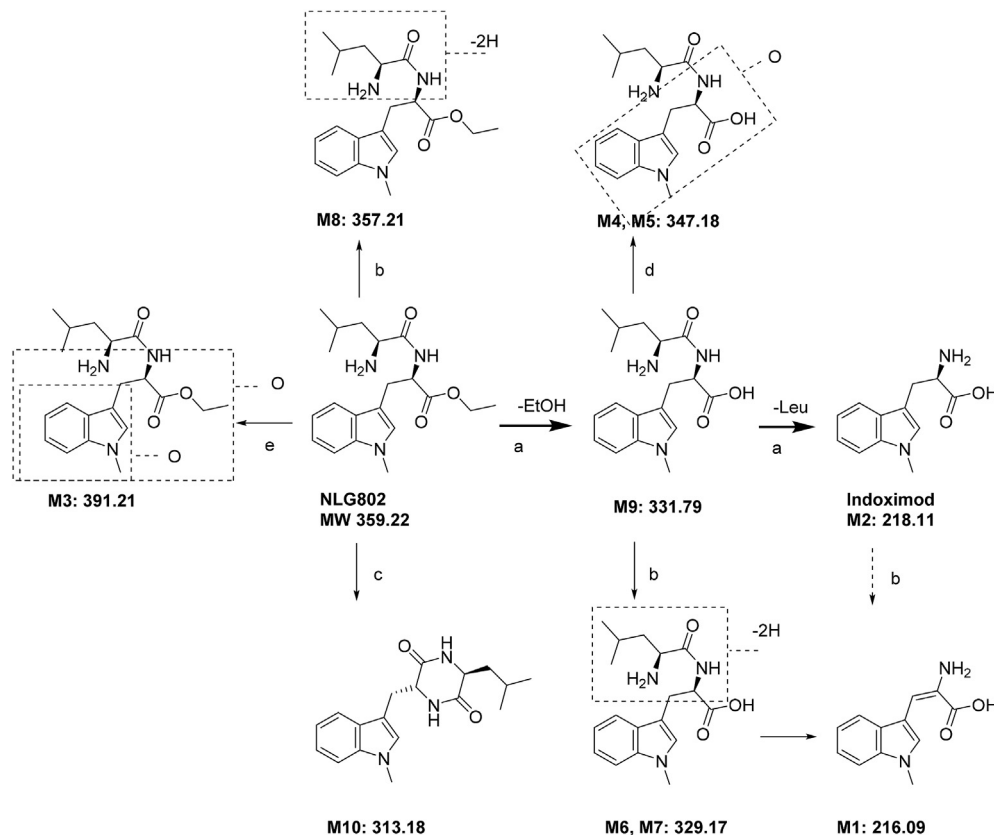


Fig. 3. Metabolic transformations for NLG802 in rat, dog, monkey and human hepatocytes. a) hydrolysis, b) dehydrogenation, c) hydrolysis and cyclization, d) oxygenation, e) oxygenation.

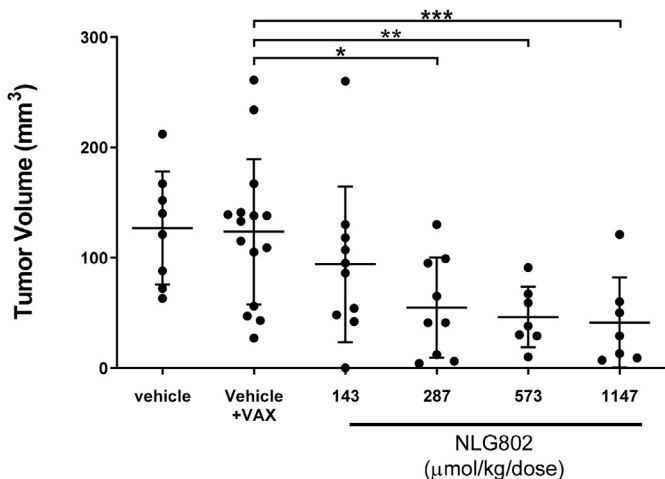


Fig. 4. Dose dependent antitumor effect of NLG802 in a murine melanoma tumor model
Fig. 4. Graphical summary of tumor measurements taken on day 11. Significance was determined using ANOVA (overall significance $p = 0.002025$) with a follow up Dunnett's multiple comparisons test comparing each dosing group against the vehicle + vaccine group (* $p = 0.0219$; ** $p = 0.0167$; *** $p = 0.00977$).

CYP450 1A2, 2B6, 2C8 and 2C9 ($IC_{50} > 50 \mu M$) and no induction of CYP1A2, 2B6 or 3A4 in human hepatocytes. NLG802 showed moderate inhibition of P-gp transporter activity in MDR1-MDCKII cells ($IC_{50} 27 \mu M$), does not inhibit the anion and cation transporters OATP1B1, OATP1B3, OAT1, OAT3, OCT1 and OCT2 in HEK293 cells expressing these transporters ($IC_{50} > 50 \mu M$) or the BRCP transporter in Caco-2 cells. Given the almost total conversion of NLG802 to downstream metabolites after absorption (Fig. 3), these weak inhibitory activities do not raise any safety concerns for potential drug interactions.

2.4.3. Pharmacokinetics of NLG802

The pharmacokinetics of NLG802 was investigated in mice, rats and monkeys, in single and repeated doses administered orally (and IV in monkeys), at doses ranging from 20 mg/kg to 900 mg/kg, in suspension or capsule formulation.

A comparative pharmacokinetic analysis was carried out in mice to bridge the dose-dependent indoximod exposure obtained after dosing indoximod or NLG802 with the known pharmacodynamic effects of indoximod in mouse models. Table 7 shows that indoximod C_{max} increases 4 to 2-fold when dosing NLG802 compared to equivalent molar doses of indoximod in the dose range of 143–1147 $\mu mol/kg$. Daily exposure (AUC_{0-24}) of indoximod observed after dosing NLG802 increases 3 and 2-fold compared with dosing indoximod at 143 and 287 $\mu mol/kg$, respectively. However, exposure values become comparable at dose levels

Table 7
 Comparison of indoximod pharmacokinetics after single dose of indoximod or NLG802 in mice.

Test Article	Dose Level	C_{max}	AUC_{0-24}	T_{max}	$T_{1/2}$
	$\mu mol/kg$	μM	$\mu M \cdot h$	h	h
Indoximod	143	9.3 ± 2.2	36.4 ± 9	0.6 (0.5–1)	3
	287	17.2 ± 3.7	77.7 ± 21.6	0.6 (0.5–1)	2.8
	573	26 ± 11.1	153.6 ± 79.2	1.0 (0.5–2)	3.1
	1147	51.7 ± 25.4	348.2 ± 115.2	1.8 (0.5–6)	3.4
NLG802	143	35 ± 25.3	105.4 ± 68.5	1.4 (0.5–2)	2.9
	287	68.9 ± 3.9	142.3 ± 64.6	0.5	2.2
	573	65.7 ± 34.1	150.8 ± 76.1	0.8 (0.5–1)	3.1
	1147	101.4 ± 38.9	374.3 ± 180.7	0.6 (0.5–1)	3.2

$>573 \mu mol/kg$ suggesting saturation pharmacokinetics above a certain dose level.

Further characterization of pharmacokinetics of NLG802 was carried out in male and female cynomolgus monkeys, after a single intravenous dose (15 mg/kg) and after single (75, 225, 675 mg/kg) and repeated (75, 150, 375 mg/kg bid) oral doses of NLG802. In these studies, quantification of the parent prodrug NLG802, as well as the intermediate metabolite M9 and the final drug indoximod were quantified in plasma (Table 8). A similar characterization was carried out in male and female rats dosed orally with NLG802 at 100–900 mg/kg bid (not shown).

In general, there were no marked sex differences in rats and monkeys. In all species, NLG802 was rapidly absorbed and extensively metabolized to the intermediate metabolite M9, which is subsequently metabolized to indoximod with T_{max} for indoximod of 1–8 h. Not all samples yielded measurable levels of NLG802 or M9 at every time point to allow calculation of all PK parameters. Metabolite to parent exposure ratios (indoximod: NLG802) were >39000 in rats and 690 to 8700 in monkeys, reflecting an extensive conversion of the NLG802 to the active drug indoximod. No drug accumulation was observed for NLG802, M9 or indoximod in rats or monkeys after repeat dose administration.

In general, half-life or clearance could not be determined for NLG802 and M9 in mice, rats or monkeys. Apparent clearance (CL/F) for NLG802 and M9 after oral dosing in monkeys was much higher than liver blood flow ($>10,000 mL/min/kg$) indicating fast conversion of NLG802 to M9 and subsequent metabolization to indoximod. In those few cases where half-life could be measured, NLG802 showed a half-life between 3 and 9.7 h and M9 showed a half-life of 3.7–8.2 h in monkeys. In general, indoximod half-life was 2.2–3.4 h in mice, 23–80 h in rats and 1.8–4.3 h in monkeys. After intravenous dosing of NLG802, clearance for indoximod in monkeys was 10 mL/min/kg and the volume of distribution (V_d) was 1 L/kg (Table 8).

Oral bioavailability could not be determined for NLG802 due to its rapid conversion to indoximod. Therefore, oral bioavailability in monkeys was measured via its conversion to indoximod after dosing of NLG802 to Cynomolgus monkeys orally at 75 mg/kg (210 $\mu mol/kg$) or intravenously at 15 mg/kg (42 $\mu mol/kg$) (Table 8). Oral bioavailability in monkeys was 61.8% and 50.1% for males and females, respectively. This compares favorably with the oral bioavailability of indoximod in male monkeys, which was determined to be 10% and 6% after oral dosing of indoximod at 275 and 825 $\mu mol/kg$, respectively (not shown). This indicates that NLG802 increases oral bioavailability of indoximod in monkeys approximately 5 to 6-fold at comparable molar dose levels.

NLG802 exhibited moderate binding ($\geq 50.0\%$ and $<95.0\%$) to plasma proteins from Beagle dog, Cynomolgus monkey and human. The bound values were non-calculable in CD-1 mouse and Sprague-Dawley rat plasma due to rapid metabolism. Metabolite M9 also exhibited a medium binding to plasma proteins from mouse, rat and monkey and was low ($<50.0\%$) in dog and human plasma.

After a single dose of NLG802 to rats at 100 mg/kg/dose, approximately 40% of the administered dose was eliminated predominantly in the urine as indoximod. After a single dose of NLG802 to monkeys at 75 mg/kg/dose, approximately 15% of the administered dose was eliminated in the urine and feces within 12 h post dose, predominantly in the urine as indoximod.

2.4.4. Toxicology of NLG802

Toxicology studies were conducted in rats (40 males and 40 females) dosed orally at 0, 20, 60, 180 (F) or 150 (M) mg/kg bid for 28 days. The severely toxic dose in 10% of the animals (STD10) was concluded to be 150 mg NLG802 free base/kg/dose bid. The C_{max} and AUC_{0-12h} for indoximod on Day 28 were 169 μM and

Table 8

Single and repeated dose pharmacokinetics of NLG802 in monkeys.

Route	Dose mg/kg	Dose μmol/kg	Analyte	Study Day	Sex	n	C _{max}	T _{max}	AUC ₀₋₂₄	T _{1/2}	CL or CL/F	Vd	
							nM	h	nM·h	h	mL/min/kg	L/kg	
IV	15	42	NLG802	1	M	1	135		63.7	NC	10918	309	
			Indoximod	1	M	3	39500 ± 2300		71800 ± 9100	2	9.8 ± 1.3	1.06	
					F	3	43100 ± 3410		70600 ± 14900	1.5	10.2 ± 2.2	0.97	
PO	75	209	NLG802	1	F	1	8.46	2	28.7	NA	121000		
				8	F	3	9.71 ± 0.874	2	35.6 ± 6.15	NA	99400 ± 16000		
					M	3	7.74 ± 2.53	1	39.7 ± 12.4	NA	92700 ± 24500		
			Indoximod	1	F	3	55000 ± 12900	2	177000 ± 93800	1.8	25.6 ± 17.5		
					M	3	74400 ± 23000	2	222000 ± 42100	3.9	16.0 ± 3.41		
				8	F	3	59300 ± 7140	1	179000 ± 15600	2.7	19.5 ± 1.64		
					M	3	47300 ± 12600	1	223000 ± 49500	2.7	16.2 ± 4.05		
					F	3	10.5 ± 2.25	1	57.0 ± 14.3	3	128000 ± 37400		
					M	3	17.1 ± 7.63	2	80.6 ± 4.88	8.5	86500 ± 5250		
PO	150	417	M9	8	M	2	192	1	305	NA	29500		
				Indoximod	8	F	3	79000 ± 8520	2	403000 ± 67500	2.7	17.6 ± 2.83	
						M	3	93400 ± 19300	2	509000 ± 58800	2.8	13.8 ± 1.70	
PO	225	626	M9	1	M	2	12.6	3	60.2	NA	227000		
				Indoximod	1	F	3	68500 ± 36500	1	181000 ± 102000	3.8	82.2 ± 66.6	
						M	3	97700 ± 29600	2	525000 ± 193000	2.9	22.1 ± 9.37	
PO	375	1043	M9	8	F	1	403	2	2400	3.4	7240		
				Indoximod	8	F	1	308	2	703	NA	24700	
						F	2	203000	2.5	1660000	3.8	24.5	
PO	675	1878	NLG802	1	F	2	75.9	1	777	5	86800		
					M	2	148	2	966	9.7	137000		
					F	2	1580	1.5	3610	8.2	20100		
			Indoximod	1	M	2	1760	1	2880	3.7	38200		
					F	3	387000 ± 506000	2	6450000 ± 9510000	10.2	111 ± 176		
					M	3	311000 ± 438000	4	4470000 ± 7170000	4.3	134 ± 184		

T_{max}: time of C_{max}; T_{1/2}: half-life; CL: clearance; CL/F: apparent clearance; Vd: volume of distribution. Average values ± SD are calculated when 3 values were available. Study Day 1 reflects PK after a single dose; Study Day 8 reflects PK after bid dosing at the stated dose level.

1410 μM h, respectively, in the males dosed at 150 mg/kg/dose bid and 170 μM and 1380 μM h, respectively, in the females dosed at 180 mg/kg bid. The no adverse effect level (NOAEL) for this study was determined to be 60 mg NLG802 free base/kg/dose bid which was associated with a C_{max} and AUC_{0-12h} of 110 μM and 953 μM h, respectively, on Day 28 for the active metabolite indoximod. Among adverse events noticed in less than 10% of animals in the highest dose group were mortality (2 due gavage errors, 2 of unknown causes), abnormal respiratory sounds, labored breathing, distended abdomen and decreased food consumption.

Additionally, a toxicology study was conducted in monkeys (12 males and 12 females) dosed orally at 0, 60, 120, 180 or 150 mg/kg bid for 28 days. The NOAEL was 120 mg/kg/dose bid, which was associated with sex averaged C_{max} of 103 μM and AUC_{0-12h} of 320 μM h for the active metabolite indoximod.

NLG802 is not genotoxic or clastogenic, does not alter behavioral parameters in rats or monkeys and does not affect cardiovascular or respiratory parameters in monkeys.

2.4.5. Pharmacodynamic activity

In order to verify that NLG802 preserves the pharmacodynamic effects of indoximod, we evaluated its antitumor effect in a mouse melanoma tumor model which involved: 1) inoculation of B16F10 tumor cells on Day 1, 2) dosing NLG802 twice a day by oral gavage from Day 6 to Day 11 at different dose levels, 3) vaccination with a gp100 vaccine on Day 7, 4) adoptive transfer of pmel-1 CD8⁺ T cells on Day 7, and 5) evaluation of tumor size on day 11. All groups of mice received adoptive transfer of pmel-1 CD8⁺ T cells. Control groups of mice were those that did not receive vaccination or did not receive NLG802 treatment. Mice were orally dosed at 143, 287, 573 and 1147 μmol/kg/dose BID. A statistically significant reduction in tumor size was obtained when mice were dosed at the doses ≥287 μmol/kg/dose (equivalent to 62 mg/kg of indoximod).

Correlating this dose with dose-dependent exposure parameters for indoximod after administration of NLG802 (Table 7) suggests that antitumor effect mediated by NLG802 takes place at daily exposures for indoximod of AUC₀₋₂₄ ≥ 290 μM h (twice the measured exposure of 145 μM h/dose due to bid dosing) and C_{max} ≥ 50 μM.

3. Conclusions

Indoximod is a clinical investigational drug candidate for the treatment of cancer intended to be administered in combination with other cancer therapies that involve stimulation of an immune response to the tumor, such as cancer immunotherapy, chemotherapy or radiotherapy. Indoximod, has been tested in human cancer clinical trials in combination with different chemotherapeutic and immunotherapeutic agents, such as docetaxel, paclitaxel, gemcitabine, nab-paclitaxel, temozolomide, idaurubicin, daunorubicin, cytarabine, ipilimumab, pembrolizumab, nivolumab, sipuleucel-T, and vaccines. Available PK data for indoximod shows a linear PK profile at doses of up to 1200 mg/dose, associated with an average daily exposure at steady state of approximately 240 μM h (i.e. C_{av,ss} 10 μM). In vitro assays and animal models suggest that different pharmacodynamics effects take place at different concentration levels, with effects on human CD4⁺ TH17 and T_{regs} taking place at lower concentrations (EC₉₀ 10 μM) while other effects such as stimulation of CD8⁺ T cell proliferation or downregulation of IDO protein expression in moDCS require higher concentrations of indoximod (EC₅₀ ≥ 30 μM). Mouse animal models suggest that increasing indoximod exposure above the currently achievable levels would improve the observed antitumor effects. The saturable dose-dependent exposure of indoximod suggested that its bioavailability is limited by absorption rather than by clearance mechanisms. Therefore, here we investigated prodrugs of indoximod designed to increase oral bioavailability of indoximod by

enhancing its intestinal absorption.

We investigated derivatization of the amino and carboxyl groups of indoximod by formation of amides, esters, carbamates or a combination of them, with protecting groups that are metabolized into molecules with a good safety profile. Since the prodrug is intended to be stable through the gastric and intestinal transit and be metabolized once entering systemic circulation, we discarded those prodrug candidates that were unstable in simulated gastric and intestinal conditions. As expected, some of the ester prodrugs showed to be unstable under these conditions. A preliminary assessment of indoximod exposure was determined by evaluation of pharmacokinetics in rats after oral dosing in solution vehicles. In general, indoximod has high bioavailability in rats (~50% depending on dose), and a long half-life (~30 h), so improvements above 2-fold in exposure parameters were not expected in this model. Since solubility and solubilization rate affects oral bioavailability, it was considered useful to test the selected candidate prodrugs in different salt forms after dosing them orally in a capsule formulation, at different dose levels. This test indicated that the best prodrugs were dipeptides, bearing a non-polar amino acid such as Leu or Met in the amino terminus, and an ethyl ester in the carboxyl terminus (**62-Cl** and **64-Cl**). These prodrugs were evaluated in monkeys, a species which has low oral bioavailability for indoximod and a similar dose-exposure profile as humans, which showed that both prodrugs increased the C_{max} and AUC, >4-fold compared to equivalent molar doses of indoximod. The selected clinical development candidate **NLG802** increased oral bioavailability to indoximod in monkeys >5-fold.

NLG802 is stable under gastric and intestinal conditions, is extensively absorbed and rapidly metabolized by carboxyl esterases (CES1b and CES1c) to a dipeptide Leu-indoximod (M9), and subsequently hydrolyzed by unidentified peptidases to individual amino acids Leu and indoximod.

The safety dose levels established in monkeys (NOAEL) were 120 mg/kg bid, which is equivalent to an allometrically equivalent dose of 3200 mg bid in humans. This dose resulted in sex averaged exposure parameters of C_{max} of 103 μ M and AUC_{0-12h} of 320 μ M h (i.e. $C_{av,ss}$ of 27 μ M) for the active metabolite indoximod. We predict that these exposure levels would bring additional therapeutic benefits for indoximod in humans.

4. Experimental section

4.1. Chemistry

All reagents and solvents were purchased from commercial sources. All commercial reagents and solvents were used as received without further purification. The reactions were monitored using analytical thin layer chromatography (TLC) with 0.25 mm EM Science silica gel plates (60F-254). The developed TLC plates were visualized by short wave UV light (254 nm) or immersion in potassium permanganate solution followed by heating on a hot plate. Flash chromatography was performed with Selecto Scientific silica gel, 32–63 μ m particle sizes. All reactions were performed in flame or oven-dried glassware under a nitrogen atmosphere. All reactions were stirred magnetically at ambient temperature unless otherwise indicated. 1H NMR spectra were obtained with a Bruker DRX400, Varian VXR400 or VXR300. 1H NMR spectra were reported in parts per million (δ) relative to TMS (0.0), DMSO- d_6 (2.50) or MeOH- d_4 (4.80) as an internal reference. All 1H NMR spectra were taken in $CDCl_3$ unless otherwise indicated. MS was conducted on Waters ACQUITY UPLC system with a QDa detector. Purity of all final target compounds was 95% or higher. High resolution mass spectrometric analysis for **NLG802** was performed on the Agilent G6224A TOF LC/MS using high performance

liquid chromatography with electrospray ionization in positive ion mode time of flight mass spectrometry (HPLC-ESI-TOF/MS).

4.1.1. Synthesis of ethyl 1-methyl-D-tryptophanate hydrochloride (**2-Cl**)

$SOCl_2$ (1.34 mL, 18.3 mmol) was added to a suspension of indoximod (4.00 g, 18.3 mmol) in ethanol (50 mL) at 0 °C and the mixture was stirred at 80 °C overnight. After cooling to rt, the solvent was distilled-off and the crude was diluted with diethyl ether (100 mL), the white solid was filtered-off and washed with dry ether (20 mL) to afford **2-Cl** (5.1 g, 98%). LCMS (ESI, m/z): 247.31 [$M + H$] $^+$. 1H NMR (DMSO- d_6): δ 1.08 (t, 3H, $J = 7.1$ Hz), 3.20–3.35 (m, 2H), 3.75 (3H, s), 4.08 (q, 2H, $J = 7.1$ Hz), 4.15 (dd, 1H, $J = 7.0$, 5.7 Hz), 7.05 (ddd, 1H, $J = 7.9$, 7.0, 1.0 Hz), 7.16 (ddd, 1H, $J = 8.2$, 7.0, 1.2 Hz), 7.22 (1H, s), 7.41 (dt, 1H, $J = 8.2$, 0.9 Hz), 7.54 (dt, 1H, $J = 7.9$, 1.0 Hz), 8.63 (br s, 3H).

4.1.2. Synthesis of isopropyl 1-methyl-D-tryptophanate hydrochloride (**3-Cl**)

$SOCl_2$ (0.167 mL, 2.29 mmol) was added to a suspension of indoximod (0.500 g, 2.29 mmol) in isopropanol (15 mL) at 0 °C rt, and the mixture was stirred at 80 °C overnight. After cooling to rt, the solvent was distilled off and the crude was basified with 25% aq $NaHCO_3$ (20 mL); the product was extracted with CH_2Cl_2 , the combined organic extract was dried over Na_2SO_4 and the solvent was distilled-off under reduced pressure. The free base was converted to its hydrochloride salt by adding dry HCl in dioxane, the solvent was removed under reduced pressure to afford **3-Cl** as white solid (0.252 g, 37%). LCMS (ESI, m/z): 261.31 [$M + H$] $^+$. 1H NMR (DMSO- d_6): δ 0.95 (d, 3H, $J = 6.3$ Hz), 1.10 (d, 3H, $J = 6.2$ Hz), 3.14–3.31 (m, 2H), 3.72 (s, 3H), 4.08 (t, 1H, $J = 6.6$ Hz), 4.79–4.85 (m, 1H), 7.00–7.04 (m, 1H), 7.12–7.18 (m, 2H), 7.39 (dd, 1H, $J = 8.5$, 2.2 Hz), 7.52 (d, 1H, $J = 7.8$ Hz), 8.51 (br s, 3H).

4.1.3. Synthesis of N^α -(tert-butoxycarbonyl)-1-methyl-D-tryptophan (**4**)

To a mixture of indoximod (3.0 g, 13.75 mmol) in dioxane (70 mL) at 0 °C, NaOH (550 mg dissolved in 30 mL DI water) was added, followed by the addition of Boc_2O . The reaction was stirred at 0 °C for 4 h and stirred overnight at rt. The solution was concentrated under reduced pressure to approx. one third the original volume. The reaction was acidified with 1 N HCl at 0 °C and the product was extracted with EtOAc (3 \times 50 mL). The organic extract was washed with brine (30 mL) and dried over Na_2SO_4 , the solvent was evaporated under reduced pressure to afford the product that was used directly in the next step without further purification (4.3 g, 98%). 1H NMR: δ 1.24 and 1.42 (2 s, 9H), 3.25–3.37 (m, 2H), 3.71 (s, 3H), 4.62–4.67 (m, 1H), 5.01–5.04 (m, 1H), 6.89 (s, 1H), 7.07–7.12 (m, 1H), 7.19–7.21 (m, 1H), 7.26–7.72 (m, 1H), 7.59 (d, 1H, $J = 7.9$ Hz).

4.1.4. Synthesis of benzyl N^α -(tert-butoxycarbonyl)-1-methyl-D-tryptophanate (**5**)

N^α -(tert-butoxycarbonyl)-1-methyl-D-tryptophan (3.00 g, 9.42 mmol) was dissolved in 60 mL of DMF, followed by the addition of Cs_2CO_3 (1.78 g, 5.47 mmol) and benzyl bromide (1.61 mL, 9.42 mmol). The resulting suspension was stirred at room temperature for 2 h. After the end of reaction (TLC), the DMF was removed under reduced pressure followed by suspending the residue in ethyl acetate (100 mL) before washing with distilled water (3 \times 50 mL) and brine. The organic layer was dried over anhydrous sodium sulfate and concentrated under vacuum. The residue was purified by column chromatography on silica gel (3.5 g, 91%). 1H NMR: δ 1.28 (s, 9H), 3.25–3.27 (m, 2H), 3.62 (s, 3H), 4.65–4.70 (m, 1H), 5.02–5.17 (m, 3H), 7.07–7.12 (m, 1H), 7.19–7.28 (m, 5H),

7.30–7.36 (m, 3H), 7.53 (d, 1H, $J = 8.0$ Hz).

4.1.5. Synthesis of benzyl 1-methyl-D-tryptophanate hydrochloride (**6-Cl**)

Ethyl acetate (26.9 mL) and MeOH (8.9 mL) in an RB flask equipped with a septum and a needle vent were cooled in an ice bath with stirring. Acetyl chloride (14.22 mL) was added slowly. The resulting solution was stirred at 0 °C for 20 min and MeOH (0.5 mL) was added. A flask containing benzyl N^α -(*tert*-butoxycarbonyl)-1-methyl-D-tryptophanate (3.5 g, 8.6 mmol) was placed in an ice bath and the cold, freshly prepared HCl (4 M in EtOAc) was slowly poured into the flask containing benzyl N^α -(*tert*-butoxycarbonyl)-1-methyl-D-tryptophanate. The solution was stirred vigorously at 0 °C for 15 min where the formation of a white suspension was observed, and the flask was removed from the ice bath. The suspension was stirred vigorously for 2.5 h. The solution was cooled in an ice bath diluted with ether (50 mL) and the suspension was filtered, and the solid cake washed with cold ether. The solid dried under high vacuum and **6-Cl** was isolated as a colorless solid (6.45 g, 88%). LCMS (ESI, m/z): 309.31 [M + H]⁺. ¹H NMR (DMSO- d_6): δ 3.28 (dd, 2H, $J = 5.6, 15.2$ Hz), 3.70 (s, 3H), 4.26–4.29 (m, 1H), 5.08 (d, 1H, $J = 12.4$ Hz), 5.13 (d, 1H, $J = 12.4$ Hz), 7.04 (t, 1H, $J = 7.6$ Hz), 7.06 (s, 1H), 7.10–7.18 (m, 3H), 7.30–7.35 (m, 3H), 7.42 (d, 1H, $J = 8.0$ Hz), 7.53 (d, 1H, $J = 8.0$ Hz).

4.1.6. General method for the derivatization of –COOH group of indoximod

DIPEA (9.42 mmol) was added to a solution of *N*-(*tert*-butoxycarbonyl)-1-methyl-D-tryptophan (3.14 mmol), the appropriate alcohol or amine (3.14 mmol) and HATU (3.14 mmol) in acetonitrile (30 mL) at 0 °C, and the solution was allowed to warm to rt. After stirring overnight (17 h), the reaction was diluted with water (50 mL) and the product was extracted with CH₂Cl₂ (3 × 50 mL). The combined organic extract was washed with water (25 mL), brine (25 mL) dried over Na₂SO₄ and concentrated under reduced pressure to afford the crude. Chromatographic purification afforded the desired product.

4.1.6.1. (2,2-Dimethyl-1,3-dioxolan-4-yl)methyl-*N*-(*tert*-butoxycarbonyl)-1-methyl-D-tryptophanate (**7**). It was obtained in 78% yield. ¹H NMR: δ 1.27 (s, 3H), 1.33 (s, 3H), 1.35 (s, 9H), 3.21 (d, 2H, $J = 5.6$ Hz), 3.44–3.50 (m, 1H), 3.67 (s, 3H), 3.80–3.86 (m, 1H), 3.99–4.03 (m, 2H), 4.07–4.12 (m, 1H), 4.58 (q, 1H, $J = 6.5$ Hz), 4.99 (d, 1H, $J = 8.2$ Hz), 6.82 (s, 1H), 7.03 (t, 1H, $J = 7.4$ Hz), 7.14 (t, 1H, $J = 7.4$ Hz), 7.21 (d, 1H, $J = 8.1$ Hz), 7.47 (d, 1H, $J = 8.0$ Hz).

4.1.6.2. (*S*)-3-(*tert*-Butoxy)-2-((*tert*-butoxycarbonyl)amino)-3-oxopropyl- N^α -(*tert*-butoxy carbonyl)-1-methyl-D-tryptophanate (**9**). It was obtained in 40% yield. ¹H NMR: δ 1.41 (s, 9H), 1.44 (s, 9H), 1.45 (s, 9H), 3.16 (dd, 1H, $J = 15.3, 4.8$ Hz), 3.29 (dd, 1H, $J = 15.3, 4.8$ Hz), 3.75 (s, 3H), 4.35–4.52 (m, 3H), 4.61 (d, 1H, $J = 6.3$ Hz), 4.99 (d, 1H, $J = 8.6$ Hz), 5.28 (d, 1H, $J = 8.7$ Hz), 6.87 (s, 1H), 7.11 (t, 1H, $J = 7.3$ Hz), 7.22 (t, 1H, $J = 7.3$ Hz), 7.29 (d, 1H, $J = 8.2$ Hz), 7.52 (d, 1H, $J = 7.8$ Hz).

4.1.6.3. *tert*-Butyl 4-(((N^α -(*tert*-butoxycarbonyl)-1-methyl-D-tryptophyl)oxy)methyl)piperidine-1-carboxylate (**11**). It was obtained in 83% yield. ¹H NMR: δ 0.93–1.10 (m, 2H), 1.29–1.32 (m, 1H), 1.45 (s, 18H), 1.63–1.69 (m, 2H), 2.59 (tt, 2H, $J = 2.4, 13.2$ Hz), 3.25 (t, 2H, $J = 5.4$ Hz), 3.75 (s, 3H), 3.84–3.92 (m, 2H), 4.01–4.06 (m, 2H), 5.06 (d, 1H, $J = 8.0$ Hz), 6.35 (br s, 1H), 6.86 (s, 1H), 7.10 (dt, 1H, $J = 1.2, 6.8$ Hz), 7.24 (dt, 1H, $J = 1.2, 6.8$ Hz), 7.28 (d, 1H, $J = 8.4$ Hz), 7.53 (d, 1H, $J = 8.0$ Hz).

4.1.6.4. *tert*-Butyl 4-(2-(((N^α -(*tert*-butoxycarbonyl)-1-methyl-D-tryptophyl)oxy)ethyl)piperidine-1-carboxylate (**13**). It was obtained in

92% yield. ¹H NMR: δ 0.95–1.05 (m, 2H), 1.47 (s, 18H), 1.32–1.40 (m, 3H), 1.55 (d, 2H, $J = 2.4$ Hz), 2.59 (dt, 2H, $J = 2.7, 12.8$ Hz), 3.25 (d, 2H, $J = 5.6$ Hz), 3.74 (s, 3H), 3.99–4.05 (m, 2H), 4.94–5.00 (m, 2H), 5.08 (d, 1H, $J = 8.0$ Hz), 6.52 (br s, 1H), 6.86 (s, 1H), 7.09 (t, 1H, $J = 7.4$ Hz), 7.21 (t, 1H, $J = 7.6$ Hz), 7.28 (d, 1H, $J = 8.0$ Hz), 7.53 (d, 1H, $J = 8.0$ Hz).

4.1.6.5. 2-(Dimethylamino)ethyl N^α -(*tert*-butoxycarbonyl)-1-methyl-D-tryptophanate (**15**). It was obtained in 38% yield. ¹H NMR: δ 1.33 (s, 1H), 1.43 (s, 8H), 2.23 (s, 5H), 2.29 (s, 1H), 2.43–2.60 (m, 4H), 3.27 (d, 2H, $J = 5.6$ Hz), 3.74 (s, 3H), 4.1–4.23 (m, 2H), 4.63 (m, 1H), 5.10 (m, 1H), 6.91 (s, 1H), 7.10 (ddd, 1H, $J = 8.0, 6.8, 1.2$ Hz), 7.21 (ddd, 1H, $J = 8.0, 6.8, 1.2$ Hz), 7.28 (d, 1H, $J = 8.0$ Hz), 7.54 (d, 1H, $J = 8.0$ Hz).

4.1.6.6. 2-(Tetrahydro-2H-pyran-4-yl)ethyl N^α -(*tert*-butoxycarbonyl)-1-methyl-D-tryptophanate (**17**). It was obtained in 60% yield. ¹H NMR: δ 1.29–1.35 (m, 2H), 1.42 (s, 9H), 1.60–1.67 (m, 5H), 3.17–3.35 (m, 4H), 3.74 (s, 3H), 3.84–3.93 (m, 2H), 4.10 (dq, 2H, $J = 10.4, 6.4$ Hz), 4.55–4.65 (m, 1H), 5.06 (d, 1H, $J = 8.2$ Hz), 6.86 (s, 1H), 7.09 (ddd, 1H, $J = 8.0, 7.0, 1.1$ Hz), 7.21 (ddd, 1H, $J = 8.2, 6.9, 1.1$ Hz), 7.28 (d, 1H, $J = 7.4$ Hz), 7.48–7.59 (m, 1H).

4.1.6.7. *tert*-Butyl N^α -(*tert*-butoxycarbonyl)-1-methyl-D-tryptophyl-L-valinate (**19**). It was obtained in 91% yield. ¹H NMR: δ 0.69 (d, 3H, $J = 6.8$ Hz), 0.75 (d, 3H, $J = 6.8$ Hz), 1.42 (s, 18H), 1.98–2.03 (m, 1H), 3.18 (dd, 1H, $J = 14.4, 7.2$ Hz), 3.27–3.35 (m, 1H), 3.73 (s, 3H), 4.35–4.39 (m, 1H), 4.50 (br s, 1H), 5.07 (br s, 1H), 6.31 (d, 1H, $J = 8.8$ Hz), 6.92 (s, 1H), 7.12 (t, 1H, $J = 7.2$ Hz), 7.22 (t, 1H, $J = 7.2$ Hz), 7.28 (d, 1H, $J = 8.0$ Hz), 7.64 (d, 1H, $J = 8.0$ Hz).

4.1.7. General method for the synthesis of carbamate esters (**21** and **22**)

The appropriate chloroformate (1.37 mmol) was added dropwise to a stirred solution of indoximod (0.150 g, 0.687 mmol) in 1:1 THF/1 M NaHCO₃ (2.75 mL, 2.75 mmol). The mixture was stirred for 30 min and the solution was diluted with water and extracted with ether 2x. The aqueous layer was cooled to 0 °C and conc. HCl solution was added to adjust the pH to ~1. The cold aqueous layer was immediately extracted with ethyl acetate and the combined organic layers were washed with water, brine and dried over Na₂SO₄. The solvent was removed under reduced pressure to afford crude the carbamate. The crude was purified by column chromatography to afford the pure carbamate.

4.1.7.1. N^α -(Ethoxycarbonyl)-1-methyl-D-tryptophan (**21**). Yield: 81%. LCMS (ESI, m/z): 291.21 [M+H]⁺. ¹H NMR: δ 1.23 (t, 3H, $J = 6.8$ Hz), 3.63–3.71 (m, 1H), 3.74 (s, 3H), 4.07–4.12 (m, 2H), 4.69 (dd, 1H, $J = 6.7, 11.6$ Hz), 5.20 (dd, 1H, $J = 6.9, 11.5$ Hz), 6.9 (s, 1H), 7.07 (t, 1H, 6.9 Hz), 7.21–7.48 (m, 2H), 7.57 (d, 1H, $J = 7.1$ Hz), 9.07 (br s, 1H).

4.1.7.2. 1-Methyl- N^α -((*neopentyl*oxy)carbonyl)-D-tryptophan (**22**). Yield: 72%. ¹H NMR: δ 0.90 (s, 9H), 3.34 (s, 2H), 3.64 (s, 3H), 3.73 (t, 1H, $J = 6.8$ Hz), 4.75 (d, 1H, $J = 7.8$ Hz), 5.23 (d, 1H, $J = 7.9$ Hz), 6.89 (s, 1H), 7.07 (t, 1H, $J = 8.2$ Hz), 7.25–7.59 (m, 2H, overlapped with CDCl₃), 7.58 (d, 1H, 7.8 Hz), 8.4 (br s, 2H).

4.1.8. General method for the derivatization of the –NH₂ group of indoximod esters

Appropriate D-tryptophanate hydrochloride ester (3.54 mmol) and appropriate acid (3.54 mmol) were stirred in acetonitrile (50 mL) at 0 °C. HATU (1.48 g, 3.89 mmol) and *i*Pr₂NEt (2.46 mL, 14.15 mmol) were added and the reaction was stirred overnight at rt. The solvent was removed under reduced pressure and the crude was diluted with water (50 mL) and dichloromethane (50 mL). The organic layer was separated, and the aqueous layer was extracted

with dichloromethane (3 × 50 mL). The combined organic layer was washed with brine (30 mL), dried over Na₂SO₄, and concentrated under reduced pressure. The crude product was purified by flash column chromatography to afford the desired product.

4.1.8.1. Ethyl N^α-((tert-butoxycarbonyl)glycyl)-1-methyl-D-tryptophanate (23). It was obtained in 94% yield. ¹H NMR: δ 1.22 (t, 3H, J = 7.2 Hz), 1.42 (s, 9H), 3.31 (d, 2H, J = 5.2 Hz), 3.72–3.77 (m, 2H), 3.74 (s, 3H), 4.07–4.17 (m, 2H), 4.86–4.91 (m, 1H), 5.04 (br s, 1H), 6.50 (d, 1H, J = 7.6 Hz), 6.86 (s, 1H), 7.10 (t, 1H, J = 7.4 Hz), 7.21 (t, 1H, J = 7.4 Hz), 7.28 (d, 1H, J = 8.0 Hz), 7.50 (d, 1H, J = 7.6 Hz).

4.1.8.2. Ethyl N^α-((tert-butoxycarbonyl)-L-alanyl)-1-methyl-D-tryptophanate (26). It was obtained in 95% yield. ¹H NMR: δ 1.20 (t, 3H, J = 7.0 Hz), 1.29 (d, 3H, J = 7.2 Hz), 1.40 (s, 9H), 3.30 (d, 1H, J = 5.6 Hz), 3.75 (s, 3H), 4.09–4.16 (m, 3H), 4.81–4.86 (m, 1H), 4.93 (br s, 1H), 6.61 (br s, 1H), 6.87 (s, 1H), 7.09 (t, 1H, J = 7.4 Hz), 7.21 (t, 1H, J = 7.6 Hz), 7.27 (d, 1H, J = 8.4 Hz, overlapped with CDCl₃), 7.52 (d, 1H, J = 8.0 Hz).

4.1.8.3. Ethyl N^α-((tert-butoxycarbonyl)-L-valyl)-1-methyl-D-tryptophanate (29). It was obtained in 95% yield. ¹H NMR: δ 0.80 (d, 3H, J = 6.8 Hz), 0.87 (d, 3H, J = 6.8 Hz), 1.19 (t, 3H, J = 7.2 Hz), 1.40 (s, 9H), 2.09–2.17 (m, 1H), 3.25–3.32 (m, 2H), 3.74 (s, 3H), 3.94–3.97 (m, 1H), 4.09–4.15 (m, 2H), 4.84–4.89 (m, 1H), 4.93–4.95 (m, 1H), 6.45 (d, 1H, J = 7.6 Hz), 6.87 (s, 1H), 7.10 (t, 1H, J = 7.4 Hz), 7.21 (t, 1H, J = 7.6 Hz), 7.27 (d, 1H, J = 7.6 Hz), 7.53 (dd, 1H, J = 8.0, 1.2 Hz).

4.1.8.4. tert-Butyl (S)-5-(((R)-1-(benzyloxy)-3-(1-methyl-1H-indol-3-yl)-1-oxopropan-2-yl)amino)-4-((tert-butoxycarbonyl)amino)-5-oxopentanoate (32). It was obtained in 93% yield. ¹H NMR: δ 1.38 (s, 9H), 1.43 (s, 9H), 1.76–1.91 (m, 1H), 1.94–2.09 (m, 1H), 2.20 (dt, 1H, J = 16.6, 7.0 Hz), 2.31 (dt, 1H, J = 16.6, 7.3 Hz), 3.19–3.36 (m, 2H), 3.67 (s, 3H), 4.90 (dt, J = 8.1, 5.6 Hz), 5.00–5.14 (m, 2H), 5.19 (s, 1H), 6.68–6.75 (m, 2H), 7.08 (ddd, 1H, J = 8.0, 6.9, 1.2 Hz), 7.18–7.28 (m, 4H), 7.29–7.37 (m, 2H), 7.50 (dt, 1H, J = 8.0, 1.0 Hz).

4.1.8.5. Ethyl N^α-((tert-butoxycarbonyl)-L-glutaminyl)-1-methyl-D-tryptophanate (35). It was obtained in 90% yield. ¹H NMR: δ 1.16 (t, 3H, J = 7.1 Hz), 1.33 (s, 9H), 1.79–1.99 (m, 2H), 2.05 (ddd, 1H, J = 15.2, 6.9, 5.7 Hz), 2.18 (ddd, 1H, J = 14.8, 8.6, 5.9 Hz), 3.21 (d, 2H, J = 5.9 Hz), 3.68 (s, 3H), 4.00–4.14 (m, 3H), 4.75 (dt, 1H, J = 7.7, 5.9 Hz), 5.22 (s, 1H), 5.55 (d, 1H, J = 7.0 Hz), 5.90 (s, 1H), 6.85 (s, 1H), 6.87–6.93 (m, 1H), 7.04 (ddd, 1H, J = 8.0, 6.9, 1.1 Hz), 7.14 (ddd, 1H, J = 8.2, 6.9, 1.1 Hz), 7.17–7.21 (m, 1H), 7.45 (d, 1H, J = 7.9 Hz).

4.1.8.6. Ethyl N^α-((tert-butoxycarbonyl)-L-isoleucyl)-1-methyl-D-tryptophanate (38). It was obtained in 93% yield. ¹H NMR: δ 0.80–0.84 (m, 6H), 1.02–0.91 (m, 2H), 1.19 (t, 3H, J = 7.1 Hz), 1.40 (s, 9H), 1.87 (m, 1H), 3.28 (t, 2H, J = 5.4 Hz), 3.72 (s, 3H), 4.00–4.04 (m, 1H), 4.05–4.16 (m, 2H), 4.85 (q, 1H, J = 6.4 Hz), 4.95 (d, 1H, J = 9.0 Hz), 6.46 (d, 1H, J = 7.7 Hz), 6.87 (s, 1H), 7.10 (ddd, 1H, J = 8.0, 6.8, 1.1 Hz), 7.20 (ddd, 1H, J = 8.2, 6.9, 1.2 Hz), 7.26 (d, 1H, J = 8.0 Hz), 7.53 (dt, 1H, J = 7.9, 1.0 Hz).

4.1.8.7. Ethyl N^α-((tert-butoxycarbonyl)-L-leucyl)-1-methyl-D-tryptophanate (41). It was obtained in 92% yield. ¹H NMR: δ 0.82–0.89 (m, 6H), 1.20 (t, 3H, J = 7.2 Hz), 1.36–1.41 (m, 1H, overlapped with Boc), 1.39 (s, 9H), 1.52–1.60 (m, 2H), 3.29 (d, 2H, J = 5.7 Hz), 3.74 (s, 3H), 4.04–4.17 (m, 3H), 4.81–4.86 (m, 2H), 6.59–6.61 (m, 1H), 6.87 (s, 1H), 7.07–7.11 (m, 1H), 7.16–7.22 (m, 1H), 7.24–7.32 (m, 1H), 7.52 (dt, 1H, J = 7.9, 1.1 Hz).

4.1.8.8. Benzyl N^α-(N²,N⁶-bis(tert-butoxycarbonyl)-L-lysyl)-1-methyl-D-tryptophanate (44). It was obtained in 91% yield. ¹H

NMR: δ 1.25 (q, 2H, J = 7.7 Hz), 1.39 (s, 9H), 1.44 (s, 9H), 1.47–1.55 (m, 1H), 1.67–1.80 (m, 2H), 3.02 (t, 2H, J = 6.7 Hz), 3.29 (d, 2H, J = 5.5 Hz), 3.66 (s, 3H), 4.04 (s, 1H), 4.53 (s, 1H), 4.90 (q, 1H, J = 6.1 Hz), 4.97 (s, 1H), 5.09 (q, 2H, J = 12.2 Hz), 6.57 (d, 1H, J = 7.8 Hz), 6.64 (s, 1H), 7.08 (t, 1H, J = 7.4 Hz), 7.20 (t, 1H, J = 7.6 Hz), 7.23–7.29 (m, 4H, overlapped with CDCl₃), 7.30–7.39 (m, 3H), 7.49 (d, 1H, J = 7.9 Hz).

4.1.8.9. Ethyl N^α-((tert-butoxycarbonyl)-L-phenylalanyl)-1-methyl-D-tryptophanate (47). It was obtained in 80% yield. ¹H NMR: δ 1.14 (t, 3H, J = 7.1 Hz), 1.29 (s, 9H), 2.82 (s, 2H), 2.91–3.02 (m, 1H), 3.03–3.10 (m, 2H), 3.25 (dd, 1H, J = 14.78, 5.2 Hz), 3.67 (s, 3H), 3.99–4.07 (m, 2H), 4.33 (br s, 1H), 4.79 (q, 1H, J = 6.2 Hz), 6.37 (d, 1H, J = 7.8 Hz), 6.57 (s, 1H), 7.06 (ddd, 1H, J = 8.0, 6.8, 1.2 Hz), 7.14–7.25 (m, 6H), 7.41 (d, 1H, J = 7.9 Hz).

4.1.8.10. Ethyl N^α-((tert-butoxycarbonyl)-L-tryptophyl)-1-methyl-D-tryptophanate (50). It was obtained in 97% yield. ¹H NMR: δ 1.12 (t, 3H, J = 7.1 Hz), 1.39 (s, 9H), 2.90 (d, 1H, J = 15.2 Hz), 3.05–3.32 (m, 3H), 3.56 (s, 3H), 3.91–4.10 (m, 2H), 4.44 (br s, 1H), 4.75 (br s, 1H), 5.15 (br s, 1H), 6.18 (d, 1H, J = 7.8 Hz), 6.27 (s, 1H), 6.86 (d, 1H, J = 2.3 Hz), 7.04 (ddd, 1H, J = 8.0, 6.8, 1.2 Hz), 7.14 (ddd, 1H, J = 8.0, 7.1, 1.2 Hz), 7.16–7.27 (m, 3H), 7.30 (dt, 1H, J = 8.1, 1.0 Hz), 7.37 (d, 1H, J = 8.2 Hz), 7.68 (d, 1H, J = 7.7 Hz), 7.80 (s, 1H).

4.1.8.11. Ethyl N^α-((tert-butoxycarbonyl)-D-tryptophyl)-1-methyl-D-tryptophanate (53). It was obtained in 97% yield. ¹H NMR: δ 1.18 (t, 3H, J = 7.1 Hz), 1.38 (s, 9H), 1.73 (br s, 1H), 3.13 (dd, 2H, J = 5.4, 2.5 Hz), 3.32 (s, 1H), 3.57 (s, 3H), 4.05 (dd, 2H, J = 17.2, 7.2 Hz), 4.43 (s, 1H), 4.72–4.80 (m, 1H), 5.07 (s, 1H), 6.22 (s, 1H), 6.42 (s, 1H), 6.90 (s, 1H), 6.97 (s, 1H), 7.04–7.25 (m, 5H), 7.33 (d, J = 8.2 Hz, 1H), 7.66 (d, J = 7.8 Hz, 1H), 7.87 (s, 1H).

4.1.8.12. Ethyl N^α-(N^α-(tert-butoxycarbonyl)-1-methyl-D-tryptophyl)-1-methyl-D-tryptophanate (56). It was obtained in 95% yield. ¹H NMR: δ 1.16 (t, 3H, J = 7.1 Hz), 1.37 (s, 9H), 3.02–3.20 (m, 3H), 3.35 (d, 1H, J = 15.0 Hz), 3.57 (s, 3H), 3.68 (s, 3H), 3.94–4.10 (m, 2H), 4.42 (br s, 1H), 4.75 (d, 1H, J = 6.8 Hz), 5.04 (s, 1H), 6.24 (br s, 1H), 6.37 (s, 1H), 6.84 (br s, 1H), 6.94 (s, 1H), 7.08–7.18 (m, 3H), 7.17–7.25 (m, 2H), 7.27–7.33 (m, 1H), 7.65 (d, 1H, J = 7.9 Hz).

4.1.8.13. Ethyl N^α-((tert-butoxycarbonyl)-L-methionyl)-1-methyl-D-tryptophanate (63). It was obtained in 84% yield. ¹H NMR: δ 1.21 (t, 3H, J = 7.2 Hz), 1.40 (s, 9H), 1.79–1.89 (m, 1H), 1.94–2.00 (m, 1H), 2.01 (s, 3H), 2.31–2.36 (m, 1H), 2.36–2.46 (m, 1H), 3.30 (dd, 2H, J = 5.7, 3.6 Hz), 3.75 (s, 3H), 4.12 (q, 2H, J = 7.2 Hz), 4.26 (d, 1H, J = 7.5 Hz), 4.84 (q, 1H, J = 6.4 Hz), 5.17 (d, 1H, J = 8.3 Hz), 6.67 (d, 1H, J = 7.2 Hz), 6.89 (s, 1H), 7.10 (t, 1H, J = 7.4 Hz), 7.21 (t, 1H, J = 7.2 Hz), 7.28 (d, 1H, J = 7.5 Hz), 7.53 (d, 1H, J = 7.9 Hz).

4.1.9. General method for the hydrolysis of substituted indoximod ethyl esters

Water (3 mL) and lithium hydroxide monohydrate (67 mg, 1.59 mmol) was added to a solution of appropriate amide (0.991 mmol) in THF (10 mL) and the mixture was stirred under ambient temperature for 2 h. The mixture was neutralized with 1 M HCl (at 0 °C) and poured into ice cold water (20 mL). The aqueous layer was extracted with EtOAc (3 × 35 mL). The combined organic layers were dried over Na₂SO₄ and concentrated. The crude product was purified by flash column chromatography to afford the desired product.

4.1.9.1. N^α-((tert-butoxycarbonyl)glycyl)-1-methyl-D-tryptophan (24). It was obtained in 83% yield. ¹H NMR: δ 1.39 (s, 9H), 3.25–3.35 (m, 2H), 3.2–3.74 (m, 5H), 4.85–4.90 (m, 1H), 5.21 (br s, 1H), 6.63

(br s, 1H), 6.90 (s, 1H), 7.08 (t, 1H, $J = 7.4$ Hz), 7.17–7.27 (m, 2H, overlapped with CDCl_3), 7.55 (d, 1H, $J = 7.6$ Hz).

4.1.9.2. N^α -((*tert*-Butoxycarbonyl)-*L*-alanyl)-1-methyl-*D*-tryptophan (**27**). It was obtained in 86% yield. $^1\text{H NMR}$: δ 1.21 (d, 3H, $J = 7.2$ Hz), 1.38 (s, 9H), 3.19–3.38 (m, 3H), 3.73 (s, 3H), 4.22–4.27 (m, 1H), 4.84 (br s, 1H), 6.77 (br s, 1H), 6.87 (s, 1H), 7.08 (t, 1H, $J = 7.4$ Hz), 7.19 (t, 1H, $J = 7.4$ Hz), 7.24 (d, 1H, $J = 8.8$ Hz, merged with chloroform), 7.57 (d, 1H, $J = 7.6$ Hz).

4.1.9.3. N^α -((*tert*-Butoxycarbonyl)-*L*-valyl)-1-methyl-*D*-tryptophan (**30**). It was obtained in 99% yield. $^1\text{H NMR}$: δ 0.77 (d, 3H, $J = 6.8$ Hz), 0.81 (d, 3H, $J = 6.4$ Hz), 1.38 (s, 9H), 1.84–1.92 (m, 1H), 3.30–3.32 (m, 1H), 3.66–3.77 (m, 4H), 4.08–4.12 (m, 1H), 4.88–4.92 (m, 1H), 5.23 (d, 1H, $J = 9.2$ Hz), 6.66 (d, 1H, $J = 7.2$ Hz), 6.92 (s, 1H), 7.09 (t, 1H, $J = 7.4$ Hz), 7.20 (t, 1H, $J = 7.6$ Hz), 7.26 (d, 1H, $J = 8.4$ Hz, overlapped with CDCl_3), 7.62 (d, 1H, $J = 8.0$ Hz).

4.1.9.4. N^α -((*tert*-Butoxycarbonyl)-*D*-glutaminyl)-1-methyl-*D*-tryptophan (**36**). It was obtained in 83% yield. $^1\text{H NMR}$: δ 1.34 (s, 9H), 1.59 (dd, 1H, $J = 14.1, 7.9$ Hz), 1.73–1.77 (m, 1H), 1.94–2.04 (m, 2H), 3.02 (dd, 1H, $J = 14.6, 7.9$ Hz), 3.13 (dd, 1H, $J = 14.5, 5.2$ Hz), 3.69 (s, 3H), 3.90–3.96 (m, 1H), 4.40–4.45 (m, 1H), 6.72 (s, 1H), 6.80 (d, 1H, $J = 8.3$ Hz), 6.96–7.02 (m, 1H), 7.05 (s, 1H), 7.10 (ddd, 1H, $J = 8.2, 7.0, 1.1$ Hz), 7.18 (s, 1H), 7.34 (d, 1H, $J = 8.2$ Hz), 7.51 (d, 1H, $J = 7.9$ Hz), 7.98 (d, 1H, $J = 7.9$ Hz), 12.70 (br s, 1H).

4.1.9.5. N^α -((*tert*-Butoxycarbonyl)-*L*-isoleucyl)-1-methyl-*D*-tryptophan (**39**). It was obtained in 92% yield. $^1\text{H NMR}$: δ 0.75–0.88 (m, 8H), 1.37 (s, 9H), 1.62–1.70 (m, 1H), 3.13–3.17 and 3.30–3.32 (two m, 2H), 3.65 and 3.70 (2 s, 3H), 4.89–4.92 (m, 1H), 5.33 (d, 1H, $J = 9.2$ Hz), 6.79 (t, 1H, $J = 7.1$ Hz), 6.92 (s, 1H), 7.08 (t, 1H, $J = 7.4$ Hz), 7.19 (t, 1H, $J = 7.7$ Hz), 7.25 (d, 1H, $J = 6.8$ Hz), 7.56 and 7.62 (2 d, 1H, $J = 8.0$ Hz).

4.1.9.6. N^α -((*tert*-Butoxycarbonyl)-*L*-leucyl)-1-methyl-*D*-tryptophan (**42**). It was obtained in 87% yield. $^1\text{H NMR}$: δ 0.76–0.96 (m, 6H), 1.39 (s, 9H), 1.40–1.54 (m, 3H), 3.29 (dd, 1H, $J = 15.1, 5.3$ Hz), 3.40 (dd, 1H, $J = 14.9, 5.7$ Hz), 3.70 (s, 3H), 4.41 (td, 1H, $J = 9.3, 5.4$ Hz), 4.86 (q, 1H, $J = 6.7, 5.8$ Hz), 5.26 (d, 1H, $J = 9.1$ Hz), 6.88 (br s, 1H), 7.05–7.11 (m, 1H), 7.14–7.28 (m, 3H), 7.59 (d, 1H, $J = 7.9$ Hz).

4.1.9.7. N^α -(N^2, N^6 -Bis(*tert*-butoxycarbonyl)-*L*-lysyl)-1-methyl-*D*-tryptophan (**45**). It was obtained in 91% yield. $^1\text{H NMR}$: δ 1.05–1.20 (m, 2H), 1.37 (s, 9H), 1.44 (s, 9H), 1.65–1.80 (m, 2H), 2.948–3.06 (m, 2H), 3.15–3.51 (m, 2H), 3.69 (s, 3H), 3.84–4.04 (m, 1H), 4.15 (d, 1H, $J = 7.6$ Hz), 4.69 (s, 1H), 4.85 (d, 1H, $J = 6.6$ Hz), 5.43 (s, 1H), 5.73–6.18 (m, 2H), 6.91 (s, 1H), 7.06 (t, 1H, $J = 7.4$ Hz), 7.18 (t, 1H, $J = 7.5$ Hz), 7.24 (d, 1H, $J = 8.3$ Hz), 7.60 (d, 1H, $J = 7.9$ Hz).

4.1.9.8. N^α -((*tert*-Butoxycarbonyl)-*L*-phenylalanyl)-1-methyl-*D*-tryptophan (**48**). It was obtained in 75% yield. $^1\text{H NMR}$: δ 1.30 (s, 9H), 2.81–2.88 (m, 1H), 2.94–3.00 (m, 1H), 3.08 (dd, 1H, $J = 14.8, 5.8$ Hz), 3.21–3.25 (m, 1H), 3.66 (s, 3H), 4.41 (d, 1H, $J = 6.7$ Hz), 4.79–4.86 (m, 1H), 5.13 (d, 1H, $J = 8.3$ Hz), 6.56 (d, 1H, $J = 6.5$ Hz), 6.63 (s, 1H), 6.95–7.25 (m, 8H), 7.46 (d, 1H, $J = 7.9$ Hz).

4.1.9.9. N^α -((*tert*-Butoxycarbonyl)-*L*-tryptophyl)-1-methyl-*D*-tryptophan (**51**). It was obtained in 91% yield. $^1\text{H NMR}$: δ 1.35 (s, 9H), 2.90–3.25 (m, 4H), 3.50 (s, 3H), 3.71–3.79 (m, 1H), 4.31–4.55 (m, 1H), 4.62–4.76 (m, 1H), 6.45 (s, 1H), 6.70–6.91 (m, 1H), 6.98–7.57 (m, 8H), 8.02 (br s, 1H).

4.1.9.10. N^α -((*tert*-Butoxycarbonyl)-*D*-tryptophyl)-1-methyl-*D*-tryptophan (**54**). It was obtained in 84% yield. $^1\text{H NMR}$: δ 1.31 (s, 9H),

3.05–3.13 (m, 3H), 3.29 (s, 1H), 3.55 (s, 3H), 4.44 (s, 1H), 4.75 (q, $J = 6.1$ Hz, 1H), 5.10 (s, 1H), 6.26 (s, 1H), 6.58 (s, 1H), 6.89 (s, 2H), 7.07–7.24 (m, 5H), 7.31 (d, 1H, $J = 8.0$ Hz), 7.64 (d, 1H, $J = 6.6$ Hz), 8.09–8.35 (m, 1H).

4.1.9.11. N^α -(N^α -((*tert*-Butoxycarbonyl)-1-methyl-*D*-tryptophyl)-1-methyl-*D*-tryptophan (**57**). It was obtained in 40% yield. $^1\text{H NMR}$: δ 1.27 (s, 9H), 2.99 (dd, 1H, $J = 14.7, 5.4$ Hz), 3.09 (dd, 1H, $J = 14.3, 6.7$ Hz), 3.16 (dd, 1H, $J = 14.8, 5.2$ Hz), 3.25–3.44 (m, 1H), 3.57 (s, 3H), 3.69 (s, 3H), 4.39 (br s, 1H), 4.76 (dt, 1H, $J = 8.1, 5.5$ Hz), 5.01 (br s, 1H), 6.29 (br s, 1H), 6.53 (s, 1H), 6.79 (br s, 1H), 6.91 (s, 1H), 6.97 (br s, 2H), 7.07–7.18 (m, 2H), 7.20 (d, 1H, $J = 8.2$ Hz), 7.21–7.34 (m, 2H, overlapped with CDCl_3), 7.62 (d, 1H, $J = 7.9$ Hz).

4.1.10. Synthesis of N^α -((*S*)-5-(*tert*-butoxy)-2-((*tert*-butoxycarbonyl)amino)-5-oxopentanoyl)-1-methyl-*D*-tryptophan (**33**)

tert-Butyl (*S*)-5-(((*R*)-1-(benzyloxy)-3-(1-methyl-1*H*-indol-3-yl)-1-oxopropan-2-yl)amino)-4-((*tert*-butoxycarbonyl)amino)-5-oxopentanoate (**32**) (800 mg, 1.38 mmol) was suspended in MeOH (8 mL) and THF (8 mL). After cooling to 0 °C, NaOH solution (2.4 mL, 2 M) was added and the reaction mixture was stirred for 1 h. The solution was acidified with 1 M HCl to pH = 4 and the solvents were concentrated under reduced pressure (40 °C). The solution was partitioned between water and DCM in a separatory funnel and the organic layer was collected. The aqueous layer was extracted with DCM (2 × 15 mL) and the combined organic layer was washed with water and brine. Chromatographic purification afforded the desired product (0.502 g, 72%). $^1\text{H NMR}$: δ 1.38 (s, 9H), 1.44 (s, 9H), 1.68–1.81 (m, 1H), 1.84–1.99 (m, 1H), 2.12–2.33 (m, 3H), 3.23–3.42 (m, 2H), 4.23 (s, 3H), 4.86 (d, 1H, $J = 6.9$ Hz), 5.41 (d, 1H, $J = 8.6$ Hz), 6.83 (d, 1H, $J = 7.5$ Hz), 6.93 (s, 1H), 7.09 (dt, 1H, $J = 8.0, 1.2$ Hz), 7.18 (t, 1H, $J = 7.8$ Hz), 7.23 (apparent d overlapped with CDCl_3 , 1H), 7.60 (d, 1H, $J = 7.9$ Hz).

4.1.11. General method for Boc deprotection

HCl solution (1.77 mL, 4.0 M solution in dioxane) was added to a solution of appropriate Boc protected amine (0.707 mmol) in dioxane (2 mL) at 0 °C. The solution was allowed to warm to rt and stirred vigorously for 2.5–18 h. The solvent was removed using rotary evaporator. The solid was diluted with dry ether (15 mL) and the product was filtered to afford the crude product. The crude was dried under high vacuum to afford the desired product.

4.1.11.1. Piperidin-4-ylmethyl 1-methyl-*D*-tryptophanate dihydrochloride (**12-Cl**). It was obtained in 50% yield. LCMS (ESI, m/z): 316.21 [$M + H$]⁺. $^1\text{H NMR}$ (DMSO- d_6): δ 1.16–1.34 (m, 2H), 1.41 (d, 1H, $J = 13.6$ Hz), 1.53 (d, 1H, $J = 13.6$ Hz), 1.61–1.66 (m, 1H), 2.66–2.70 (m, 2H), 3.08–3.16 (m, 2H), 3.22–3.28 (m, 1H), 3.36–3.44 (m, 1H), 3.74 (s, 3H), 3.78–3.88 (m, 2H), 4.12–4.17 (m, 1H), 7.05 (t, 1H, $J = 7.4$ Hz), 7.15 (t, 1H, $J = 7.4$ Hz), 7.24 (s, 1H), 7.40 (d, 1H, $J = 8.0$ Hz), 7.55 (d, 1H, $J = 7.6$ Hz), 8.83 (br s, 3H), 9.06 (br s, 1H), 9.34 (br s, 1H).

4.1.11.2. 2-(Piperidin-4-yl)ethyl 1-methyl-*D*-tryptophanate dihydrochloride (**14-Cl**). It was obtained in 64% yield. LCMS (ESI, m/z): 330.41 [$M + H$]⁺. $^1\text{H NMR}$ (DMSO- d_6): δ 1.24–1.45 (m, 5H), 1.60 (d, 2H, $J = 13.2$ Hz), 2.64–2.72 (m, 2H), 3.11–3.14 (m, 2H), 3.25 (dd, 1H, $J = 14.4, 7.6$ Hz), 3.33–3.83 (m, 1H, merged with H_2O from DMSO), 3.75 (s, 3H), 3.99–4.08 (m, 2H), 4.15 (t, 1H, $J = 6.6$ Hz), 7.04 (t, 1H, $J = 7.4$ Hz), 7.16 (t, 1H, $J = 7.6$ Hz), 7.24 (s, 1H), 7.42 (d, 1H, $J = 8.0$ Hz), 7.53 (d, 1H, $J = 8.0$ Hz), 8.75 (br s, 3H), 8.95 (br s, 1H), 9.16 (br s, 1H).

4.1.11.3. 2-(Dimethylamino)ethyl 1-methyl-*D*-tryptophanate dihydrochloride (**16-Cl**). It was obtained in 42% yield. LCMS (ESI, m/z):

289.4 [M + H]⁺. ¹H NMR (MeOH-d₄): δ 2.69 (s, 3H), 2.77 (s, 3H), 3.30–3.31 (m, 4H), 3.46 (dd, 2H, J = 6.7, 2.1 Hz), 3.81 (s, 3H), 4.33–4.38 (m, 1H), 4.46 (t, 1H, J = 6.6 Hz), 4.51–4.57 (m, 1H), 7.09–7.13 (m, 1H), 7.20–7.24 (m, 2H), 7.40 (d, 1H, J = 8.0 Hz), 7.58 (d, 1H, J = 8.0).

4.1.11.4. 2-(Tetrahydro-2H-pyran-4-yl)ethyl 1-methyl-D-tryptophanate hydrochloride (**18-Cl**). It was obtained in 94% yield. LCMS (ESI, m/z): 331.41 [M + H]⁺. ¹H NMR (DMSO-d₆): δ 0.93–1.11 (m, 2H), 1.18 (d, 1H, J = 6.2 Hz), 1.26–1.43 (m, 4H), 3.14 (d, 2H, J = 11.2 Hz), 3.23 (dd, 1H, J = 14.7, 7.7 Hz), 3.29–3.39 (m, 2H), 3.69–3.78 (m, 4H), 4.04 (d, 2H, J = 6.2 Hz), 4.17 (t, 1H, J = 6.6 Hz), 7.04 (ddd, 1H, J = 8.0, 7.1, 1.0 Hz), 7.16 (ddd, 1H, J = 8.3, 7.0, 1.2 Hz), 7.23 (s, 1H), 7.42 (d, 1H, J = 8.2 Hz), 7.53 (dd, 1H, J = 8.1, 1.4 Hz), 8.69 (br s, 3H).

4.1.11.5. 1-Methyl-D-tryptophyl-L-valine hydrochloride (**20-Cl**). It was obtained in 40% yield. LCMS (ESI, m/z): 378.42 [M + H]⁺. ¹H NMR (DMSO-d₆): δ 0.71–0.77 (m, 6H), 1.91–2.00 (m, 1H), 3.08 (dd, 1H, J = 14.4, 8.4 Hz), 3.23 (dd, 1H, J = 14.4, 8.4 Hz), 3.73 (s, 3H), 4.12–4.17 (m, 2H), 7.06 (t, 1H, J = 7.4 Hz), 7.17 (t, 1H, J = 7.8 Hz), 7.20 (s, 1H), 7.40 (d, 1H, J = 8.4 Hz), 7.74 (d, 1H, J = 8.0 Hz), 8.2 (br s, 3H), 8.74 (d, 1H, J = 8.4 Hz).

4.1.11.6. N^α-Glycyl-1-methyl-D-tryptophan hydrochloride (**25-Cl**). It was obtained in 87% yield. LCMS (ESI, m/z): 276.31 [M + H]⁺. ¹H NMR (DMSO-d₆): δ 3.02–3.08 (m, 1H), 3.17–3.22 (m, 1H), 3.48–3.60 (m, 2H), 3.74 (s, 3H), 4.55–4.58 (m, 1H), 7.03 (t, 1H, J = 7.8 Hz), 7.12–7.18 (m, 2H), 7.38 (d, 1H, J = 8.0 Hz), 7.55 (d, 1H, J = 8.0 Hz), 8.13 (br s, 3H), 8.76 (d, 1H, J = 8.0 Hz), 12.87 (br s, 1H).

4.1.11.7. N^α-(L-Alanyl)-1-methyl-D-tryptophan hydrochloride (**28-Cl**). It was obtained in 44% yield. LCMS (ESI, m/z): 290.31 [M + H]⁺. ¹H NMR (DMSO-d₆): δ 1.18 (d, 3H), 3.02–3.06 (m, 1H), 3.17–3.23 (m, 1H), 3.72 (s, 3H), 4.05–4.09 (m, 1H), 4.57–4.62 (m, 1H), 7.02 (t, 1H, J = 7.6 Hz), 7.12–7.15 (m, 2H), 7.38 (d, 1H, J = 8.0 Hz), 7.52 (d, 1H, J = 7.6 Hz), 8.16 (br s, 3H), 8.88–8.92 (m, 1H).

4.1.11.8. N^α-(L-Valyl)-1-methyl-D-tryptophan hydrochloride (**31-Cl**). It was obtained in 92% yield. LCMS (ESI, m/z): 318.42 [M + H]⁺. ¹H NMR (DMSO-d₆): δ 0.54 (d, 3H, J = 7.2 Hz), 0.72 (d, 3H, J = 6.8 Hz), 1.89–1.94 (m, 1H), 3.01 (dd, 1H, J = 14.8, 9.6 Hz), 3.22 (dd, 1H, J = 14.6, 5.0 Hz), 3.56–3.65 (m, 1H), 3.70 (s, 3H), 4.61–4.66 (m, 1H), 7.01 (t, 1H, J = 7.6 Hz), 7.12 (s, 1H), 7.12 (t, 1H, J = 7.6 Hz), 7.36 (t, 1H, J = 8.0 Hz), 7.56 (d, 1H, J = 8.0 Hz), 8.09 (br s, 3H), 8.78 (d, 1H, J = 8.4 Hz), 12.8 (br s, 1H).

4.1.11.9. (S)-4-Amino-5-(((R)-1-carboxy-2-(1-methyl-1H-indol-3-yl)ethyl)amino)-5-oxopentanoic acid hydrochloride (**34-Cl**). It was obtained in 85% yield. LCMS (ESI, m/z): 348.42 [M + H]⁺. ¹H NMR (DMSO-d₆): δ (mixture of rotamers) 1.73–2.21 (m, 4H), 2.93–3.12 (m, 1H), 3.14–3.27 (m, 1H), 3.70 (s, 3H), 3.83 (q, 1H, J = 5.8 Hz), 4.53–4.72 (m, 1H), 7.01 (tt, 1H, J = 7.3, 3.7 Hz), 7.07–7.19 (m, 2H), 7.35 (dt, 1H, J = 7.5, 3.5 Hz), 7.44–7.61 (m, 1H), 8.42 (br s, 3H), 8.83–9.10 (m, 1H).

4.1.11.10. N^α-(L-Glutaminyl)-1-methyl-D-tryptophan hydrochloride (**37-Cl**). It was obtained in 97% yield. LCMS (ESI, m/z): 347.32 [M + H]⁺. ¹H NMR (DMSO-d₆): δ 1.79–1.84 (m, 2H), 1.95–2.06 (m, 2H), 3.04 (dd, 1H, J = 14.6, 8.5 Hz), 3.19 (dd, 1H, J = 14.6, 5.2 Hz), 3.49–3.35 (m, 2H), 3.70 (s, 3H), 3.78–3.88 (m, 1H), 4.53 (td, 1H, J = 8.3, 5.2 Hz), 6.93 (s, 1H), 7.00 (ddd, 1H, J = 8.0, 7.0, 1.0 Hz), 7.16–7.07 (m, 2H), 7.35 (dt, 1H, J = 8.3, 0.9 Hz), 7.38 (s, 1H), 7.54 (dt, 1H, J = 7.9, 1.0 Hz), 8.28 (d, 2H, J = 4.2 Hz), 8.87 (d, 1H, J = 8.1 Hz).

4.1.11.11. N^α-(L-Isoleucyl)-1-methyl-D-tryptophan hydrochloride (**40-Cl**). It was obtained in 94% yield. LCMS (ESI, m/z): 332.41 [M + H]⁺. ¹H NMR (DMSO-d₆): δ 0.55–0.65 (m, 6H), 0.71–0.75 (m, 1H), 1.03–1.12 (m, 1H), 1.57–1.63 (m, 1H), 2.99 (dd, 1H, J = 14.6, 9.8 Hz), 3.19 (dd, 1H, J = 14.6, 4.7 Hz), 3.61–3.63 (m, 1H), 3.69 (s, 3H), 4.58–4.64 (m, 1H), 7.0 (t, 1H, J = 7.6 Hz), 7.08–7.13 (m, 2H), 7.35 (d, 1H, J = 8.2 Hz), 7.53 (d, 1H, J = 7.9 Hz), 8.10 (br s, 3H), 8.72 (d, 1H, J = 8.1 Hz).

4.1.11.12. N^α-(L-Leucyl)-1-methyl-D-tryptophan hydrochloride (**43-Cl**). It was obtained in 95% yield. LCMS (ESI, m/z): 332.31 [M + H]⁺. ¹H NMR (DMSO-d₆): δ 0.68 (t, 6H, J = 5.5 Hz), 1.17–1.34 (m, 3H), 2.99 (dd, 1H, J = 14.5, 9.6 Hz), 3.20 (dd, 1H, J = 14.6, 4.7 Hz), 3.34–3.40 (m, 3H), 3.68 (s, 3H), 4.52–4.62 (m, 1H), 6.99 (t, 1H, J = 7.4 Hz), 7.08–7.16 (m, 2H), 7.35 (d, 1H, J = 8.2 Hz), 7.54 (d, 1H, J = 7.9 Hz), 8.17 (br s, 2H), 8.85 (d, 1H, J = 8.3 Hz).

4.1.11.13. N^α-(L-Lysyl)-1-methyl-D-tryptophan dihydrochloride (**46-Cl**). It was obtained in 87% yield. LCMS (ESI, m/z): 347.42 [M + H]⁺. ¹H NMR (DMSO-d₆): δ 0.88–1.13 (m, 2H), 1.33–1.56 (m, 4H), 2.54 (t, 2H, J = 7.1 Hz), 2.95–3.10 (m, 1H), 3.15–3.24 (m, 1H), 3.42 (apparent q overlapping with H₂O, 1H, J = 7.0 Hz), 3.73 (s, 3H), 4.50–4.67 (m, 1H), 7.01 (t, 1H, J = 7.5 Hz), 7.06–7.18 (m, 2H), 7.38 (d, 1H, J = 8.3 Hz), 7.55 (d, 1H, J = 7.9 Hz), 8.02 (br s, 3H), 8.20 (br s, 3H), 8.83 (d, 1H, J = 8.1 Hz), 12.93 (br s, 1H).

4.1.11.14. N^α-(L-Phenylalanyl)-1-methyl-D-tryptophan hydrochloride (**49-Cl**). It was obtained in 91% yield. LCMS (ESI, m/z): 366.32 [M + H]⁺. ¹H NMR (DMSO-d₆): δ 2.78 (dd, 1H, J = 13.9, 7.1 Hz), 2.89–2.97 (m, 2H), 3.10 (dd, 1H, J = 14.5, 5.3 Hz), 3.35 (br s, 3H), 3.47 (s, 3H), 4.05 (dd, 1H, J = 7.1, 5.6 Hz), 4.51 (td, 1H, J = 8.2, 5.3 Hz), 6.92–6.94 (m, 2H), 6.99–7.18 (m, 6H), 7.36 (dt, 1H, J = 8.3, 0.9 Hz), 7.56 (dt, J = 8.0, 0.9 Hz, 1H), 8.89 (d, 1H, J = 8.1 Hz).

4.1.11.15. N^α-(L-Tryptophyl)-1-methyl-D-tryptophan hydrochloride (**52-Cl**). It was obtained in 90% yield. LCMS (ESI, m/z): 405.42 [M + H]⁺. ¹H NMR (DMSO-d₆): δ 2.88 (dd, 1H, J = 14.7, 8.2 Hz), 2.98 (dd, 1H, J = 14.5, 7.9 Hz), 3.08 (dt, 2H, J = 14.7, 5.0 Hz), 3.63 (s, 3H), 4.06 (br s, 1H), 4.55 (q, 1H, J = 7.9), 6.87 (dd, 1H, J = 8.0, 7.0 Hz), 6.97 (s, 1H), 7.01 (t, 1H, J = 7.4 Hz), 7.06 (t, 1H, J = 7.4 Hz), 7.08–7.15 (m, 2H), 7.34 (d, 2H, J = 8.2 Hz), 7.56 (dd, 2H, J = 8.0, 5.1 Hz), 8.09 (s, 3H), 8.95 (d, 1H, J = 8.1 Hz), 11.02 (s, 1H).

4.1.11.16. N^α-(D-Tryptophyl)-1-methyl-D-tryptophan hydrochloride (**55-Cl**). It was obtained in 95% yield. LCMS (ESI, m/z): 405.42 [M+H]⁺. ¹H NMR (Methanol-d₄): δ 3.15 (d, 1H, J = 8.5 Hz), 3.19 (d, 1H, J = 8.5 Hz), 3.36 (d, 1H, J = 4.9 Hz), 3.37–3.41 (m, 1H), 3.71 (s, 3H), 4.06 (t, 1H, J = 3.6 Hz), 4.74 (s, 1H), 6.93 (s, 1H), 7.02 (t, 1H, J = 6.2 Hz), 7.04–7.07 (m, 1H), 7.14 (td, 2H, J = 7.9, 1.7 Hz), 7.20 (s, 1H), 7.22 (d, J = 8.1 Hz, 1H), 7.30 (d, 1H, J = 8.2 Hz), 7.38 (d, 1H, J = 8.1 Hz), 7.56 (d, 1H, J = 8.0 Hz), 7.65 (d, 1H, J = 7.9 Hz), 7.70 (d, 1H, J = 8.2 Hz).

4.1.11.17. 1-Methyl-N^α-(1-methyl-D-tryptophyl)-D-tryptophan hydrochloride (**58-Cl**). It was obtained in 92% yield. LCMS (ESI, m/z): 419.42 [M + H]⁺. ¹H NMR (DMSO-d₆): δ 3.10 (td, 2H, J = 15.5, 7.9 Hz), 3.24 (ddd, 2H, J = 17.5, 15.1, 5.9 Hz), 3.72 (s, 2H), 3.73 (s, 4H), 4.02 (dd, 1H, J = 8.3, 5.1 Hz), 4.58 (q, 1H, J = 7.0 Hz), 7.04 (td, 2H, J = 7.4, 4.2 Hz), 7.09–7.23 (m, 4H), 7.40 (t, 2H, J = 8.1 Hz), 7.58 (d, 1H, J = 7.9 Hz), 7.74 (d, 1H, J = 7.9 Hz), 8.11 (s, 1H), 8.97 (d, 1H, J = 7.7 Hz), 12.82 (br s, 1H).

4.1.11.18. Ethyl N^α-(L-glutaminyl)-1-methyl-D-tryptophanate hydrochloride (**59-Cl**). It was obtained in 59% yield. LCMS (ESI, m/z): 375.42 [M + H]⁺. ¹H NMR (DMSO-d₆): δ 1.08 (t, 3H,

$J = 7.1$ Hz), 1.81–1.97 (m, 2H), 2.01–2.12 (m, 2H), 3.07 (dd, 1H, $J = 14.4, 8.4$ Hz), 3.16 (dd, 1H, $J = 14.4, 6.0$ Hz), 3.70 (s, 3H), 3.82 (t, 1H, $J = 6.0$ Hz), 4.03 (q, 2H, $J = 7.1$ Hz), 4.53 (q, 1H, $J = 7.0$ Hz), 6.93 (s, 1H), 7.02 (ddd, 1H, $J = 7.9, 7.0, 1.0$ Hz), 7.09–7.14 (m, 2H), 7.35 (d, 1H, $J = 8.2$ Hz), 7.40 (s, 1H), 8.24 (br s, 3H), 9.01 (d, 1H, $J = 7.2$ Hz).

4.1.11.19. Ethyl N^α -(*L*-isoleucyl)-1-methyl-*D*-tryptophanate hydrochloride (**60-Cl**). It was obtained in 93% yield. LCMS (ESI, m/z): 360.42 $[M + H]^+$. 1H NMR (DMSO- d_6): δ 0.60–0.66 (m, 6H), 0.75–0.82 (m, 2H), 1.12 (t, 3H, $J = 7.1$ Hz, 4H), 1.63 (br s, 1H), 3.02 (dd, 1H, $J = 14.6, 9.4$ Hz), 3.17 (dd, 1H, $J = 14.6, 5.2$ Hz), 3.61 (br s, 1H), 3.69 (s, 3H), 4.07 (q, 2H, $J = 7.1$ Hz), 4.62 (br s, 1H), 7.01 (t, 1H, $J = 7.5$ Hz), 7.10–7.14 (m, 2H), 7.36 (d, 1H, $J = 8.2$ Hz), 7.49 (d, 1H, $J = 7.9$ Hz), 8.00 (br s, 2H), 8.85 (br s, 1H).

4.1.11.20. Ethyl N^α -(*L*-phenylalanyl)-1-methyl-*D*-tryptophanate hydrochloride (**61-Cl**). It was obtained in 60% yield. LCMS (ESI, m/z): 394.42 $[M + H]^+$. 1H NMR (DMSO- d_6): δ 1.15 (t, 3H, $J = 7.1$ Hz), 2.52 (dd, 1H, $J = 13.7, 9.9$ Hz), 3.17–3.23 (m, 3H), 3.46 (dd, 1H, $J = 9.9, 4.1$ Hz), 3.64 (s, 3H), 4.03–4.11 (m, 2H), 4.83 (dt, 1H, $J = 8.4, 5.6$ Hz), 6.72 (s, 1H), 6.99 (ddd, 1H, $J = 8.0, 6.9, 1.1$ Hz), 7.31–7.05 (m, 7H), 7.45 (d, 1H, $J = 7.9$ Hz), 7.61 (d, 1H, $J = 8.4$ Hz).

4.1.11.21. Ethyl N^α -(*L*-leucyl)-1-methyl-*D*-tryptophanate hydrochloride (**62-Cl**, **NLG802**). It was obtained in 93% yield. HRMS (ESI, m/z): $[M + H]^+$ calculated for $C_{20}H_{30}N_3O_3^+$, 360.2282; found 360.2283. Elemental analysis: C 60.67%, H 7.71%, N 10.71%, Cl 8.98%. 1H NMR (DMSO- d_6): δ 0.73 (t, 6H, $J = 5.7$ Hz), 1.16 (t, 3H, $J = 7.1$ Hz), 1.23–1.37 (m, 3H), 3.03 (dd, 1H, $J = 14.5, 9.4$ Hz), 3.20 (dd, 1H, $J = 14.5, 5.3$ Hz), 3.72 (s, 4H), 4.10 (q, 2H, $J = 7.1$ Hz), 4.57–4.62 (m, 1H), 7.0–7.04 (m, 1H), 7.12–7.16 (m, 2H), 7.38 (d, 1H, $J = 8.2$ Hz), 7.52 (d, 1H, $J = 7.9$ Hz), 8.20 (3H, s), 9.01 (d, 1H, $J = 8.1$ Hz). ^{13}C NMR (100 MHz, DMSO- d_6): δ 14.0, 22.0, 22.3, 23.3, 27.0, 32.3, 50.7, 53.2, 60.7, 108.5, 109.6, 118.2, 118.6, 121.1, 127.3, 128.5, 136.6, 169.0, 171.3.

4.1.11.22. Ethyl N^α -(*L*-methionyl)-1-methyl-*D*-tryptophanate hydrochloride (**64-Cl**). It was obtained in 90% yield. LCMS (ESI, m/z): 378.42 $[M + H]^+$. 1H NMR (DMSO- d_6): δ 1.69 (t, 3H, $J = 7.1$ Hz), 2.44 (s, 3H), 2.61–2.82 (m, 2H), 3.59 (dd, 1H, $J = 14.5, 9.5$ Hz), 3.74 (dd, 1H, $J = 14.6, 5.0$ Hz), 4.27 (s, 3H), 4.37 (s, 1H), 4.63 (q, 2H, $J = 7.1$ Hz), 5.05–5.22 (m, 1H), 7.56 (t, 1H, $J = 7.4$ Hz), 7.62–7.75 (m, 2H), 7.91 (d, 1H, $J = 8.2$ Hz), 8.05 (d, 1H, $J = 7.8$ Hz), 8.86 (s, 2H), 9.60 (d, 1H, $J = 7.8$ Hz).

4.1.12. Synthesis of 2,3-dihydroxypropyl 1-methyl-*D*-tryptophanate hydrochloride (**8-Cl**)

TFA (16.3 mL, 212.7 mmol) and water (0.958 g, 53.18 mmol) was added to a solution of **7** (11.5 g, 26.59 mmol) in THF (100 mL) at 0 °C, the cooling bath was removed, and the mixture was stirred at rt for 2 h. HCl (13.3 mL, 53.18 mmol; 4.0 M solution in dioxane) was added and continued stirring for 1 h. The reaction was stirred at 40 °C for 45 min. The precipitated white solid was filtered and washed with MTBE to afford **8-Cl** (4.5 g, 51%). LCMS (ESI, m/z): 293.31 $[M + H]^+$. 1H NMR (DMSO- d_6): δ 3.32–3.40 (m, 1H), 3.44–3.52 (m, 3H), 3.76–3.86 (m, 4H), 4.16–4.37 (m, 3H), 7.10 (t, 1H, $J = 7.4$ Hz), 7.14 (s, 1H), 7.19 (t, 1H, $J = 7.6$ Hz), 7.38 (d, 1H, $J = 8.2$ Hz), 7.58 (d, 1H, $J = 7.9$ Hz).

4.1.13. Synthesis of *O*-(1-methyl-*D*-tryptophyl)-*L*-serine dihydrochloride (**10-Cl**)

HCl (2 mL, 4 M solution in dioxane) was added to a solution of **9** (0.450 g, 824.66 mmol) in CH_2Cl_2 (10 mL) at 0 °C and the solution was allowed to warm to rt. After stirring for 5 h, the solvent was evaporated, and the reaction was diluted with trifluoroacetic acid (8 mL) and the solution was stirred for 7 h at rt. After evaporating

trifluoroacetic acid the reaction mixture was diluted with dry HCl solution (1 mL, 4 M solution in dioxane) and the mixture was stirred for 10 min. The solvent was evaporated under reduced pressure, the product was triturated with ethanol:ether (10:90, 15 mL) and the product was filtered and washed with dry ether (10 mL). The product was dried under reduced pressure to afford **10-Cl** (0.190 g, 61%). LCMS (ESI, m/z): 306.31 $[M + H]^+$. 1H NMR (MeOH- d_4): δ 3.22–3.28 (m, 1H), 3.43 (dd, 1H, $J = 15.4, 4.7$ Hz), 3.70 (s, 3H), 4.23 (t, 1H, $J = 3.9$ Hz), 4.35 (dd, 1H, $J = 8.0, 4.9$ Hz), 4.60 (d, 2H, $J = 3.8$ Hz), 6.99–7.04 (m, 1H), 7.05 (s, 1H), 7.09–7.16 (m, 1H), 7.29 (d, 1H, $J = 8.3$ Hz), 7.50 (d, 1H, $J = 7.9$ Hz).

4.1.14. General method for the generation of free base form of indoximod prodrugs

Conditions A: Appropriate prodrug **8-Cl**, **12-Cl**, **59-Cl**, **62-Cl** or **64-Cl**, (1.25 mmol) was stirred in aqueous saturated $NaHCO_3$ (25 mL) solution for 5–10 min at 0 °C and the product was extracted with CH_2Cl_2 (3 \times 35 mL) or $CF_3CH_2OH:CH_2Cl_2$ (5:95; 3 \times 35 mL). The combined organic extract was dried over Na_2SO_4 and concentrated to afford the desired free base.

Conditions B: **25-Cl** and **46-Cl** were converted to the corresponding free bases with Dowex sulfonic acid resin. The compound was eluted with 20% aqueous NH_4OH solution and the aqueous solution was concentrated under reduced pressure, the crude was co-evaporated with ethanol three times to yield the desired free base.

4.1.15. General method for the generation of mono and di phosphate salts of indoximod prodrugs

To a solution of prodrug in its free base form (0.747 mmol) in EtOH (5 mL) at 0 °C, was added phosphoric acid (0.747 mmol; a solution in EtOH 1 mL) or (1.494 mmol in case of diamine) and the mixture was allowed to warm to RT and stirred for 5–18 h. The solvent was removed under reduced pressure and the residue was diluted with methyl *tert*-butylether (10 mL), after stirring for 1–5 h the solid was filtered and dried under reduced pressure to afford the desired product.

4.1.15.1. (*2R*)-1-(2,3-Dihydroxypropoxy)-3-(1-methyl-1*H*-indol-3-yl)-1-oxopropan-2-aminium dihydrogen phosphate (**8-P**). Obtained with 44% yield. 1H NMR (DMSO- d_6): δ 3.07–3.15 (m, 2H), 3.27–3.38 and 3.43–3.50 (m, 2H), 3.60–3.68 (m, 1H), 3.73 (s, 3H), 3.84 (br s, 1H), 3.90–3.96 (m, 1H), 4.02–4.12 (m, 1H), 6.95 (br s, 3H), 7.02 (ddd, 1H, $J = 8.0, 7.0, 1.0$ Hz), 7.11–7.19 (m, 2H), 7.38 (dt, 1H, $J = 8.3, 0.9$ Hz), 7.49–7.56 (m, 1H).

4.1.15.2. Piperidin-4-ylmethyl 1-methyl-*D*-tryptophanate dihydrogen phosphate (**12-P**). Obtained with 79% yield. 1H NMR (DMSO- d_6): δ 1.35–1.56 (m, 4H), 1.63–1.68 (m, 1H), 2.61–2.73 (m, 2H), 3.09–3.26 (m, 4H), 3.73 (s, 3H), 3.81 (dd, 1H, $J = 5.1, 10.9$ Hz), 3.88 (dd, 1H, $J = 5.1, 11.1$ Hz), 3.95 (t, 1H, $J = 6.7$ Hz), 7.02 (t, 1H, $J = 7.4$ Hz), 7.09–7.17 (m, 1H), 7.21 (s, 1H), 7.38 (d, 1H, $J = 8.2$ Hz), 7.49 (d, 1H, $J = 7.9$ Hz), 8.44 (br s, 10H).

4.1.15.3. (*R*)-2-((1-Carboxy-2-(1-methyl-1*H*-indol-3-yl)ethyl)amino)-2-oxoethan-1-aminium dihydrogen phosphate (**25-P**). Obtained with 80% yield. 1H NMR (DMSO- d_6): δ 3.01–3.05 (m, 1H), 3.18–3.22 (m, 1H), 3.42–3.56 (m, 2H), 3.72 (s, 3H), 4.42–4.50 (m, 1H), 7.01–7.14 (m, 3H), 7.33–7.37 (m, 1H), 7.51–7.55 (m, 1H), 8.44 (br s, 9H), 8.65 (s, 1H).

4.1.15.4. (*S*)-6-(((*R*)-1-Carboxy-2-(1-methyl-1*H*-indol-3-yl)ethyl)amino)-6-oxohexane-1,5-diaminium dihydrogen phosphate (**46-P**). Obtained with 81% yield. 1H NMR (D_2O): δ 0.39–0.78 (m, 2H), 1.21 (ddd, 2H, $J = 9.1, 6.8, 2.6$ Hz), 1.28–1.49 (m, 2H), 2.39 (td, 2H, $J = 7.4,$

3.8 Hz), 3.08 (dd, 1H, $J = 15.0, 10.9$ Hz), 3.45 (ddd, 1H, $J = 15.1, 4.5, 1.0$ Hz), 3.74 (s, 3H), 3.79 (t, 1H, $J = 6.7$ Hz), 4.68–4.77 (m, 1H), 7.14 (d, 1H, $J = 0.8$ Hz), 7.14–7.20 (m, 1H), 7.28 (ddd, 1H, $J = 8.3, 7.1, 1.1$ Hz), 7.41–7.47 (m, 1H), 7.70 (dd, 1H, $J = 7.9, 0.9$ Hz).

4.1.15.5. (*S*)-5-Amino-1-(((*R*)-1-ethoxy-3-(1-methyl-1*H*-indol-3-yl)-1-oxopropan-2-yl)amino)-1,5-dioxopentan-2-aminium dihydrogen phosphate (**59-P**). Obtained with 59% yield. $^1\text{H NMR}$ (DMSO- d_6): δ 1.10 (t, 3H, $J = 7.0$ Hz), 1.64–1.70 (m, 1H), 1.75–1.85 (m, 1H), 2.06 (t, 2H, $J = 7.9$ Hz), 3.06–3.18 (m, 2H), 3.44 (br s, 1H), 3.72 (s, 3H), 4.04 (q, 2H, $J = 7.1$ Hz), 4.52 (q, 1H, $J = 7.1$ Hz), 6.80 (s, 1H), 7.02 (t, 1H, $J = 7.5$ Hz), 7.11–7.16 (m, 2H), 7.32–7.38 (m, 2H), 7.50 (d, 1H, $J = 7.9$ Hz), 7.82 (br s, 3H), 8.57 (s, 1H).

4.1.15.6. (*S*)-1-(((*R*)-1-Ethoxy-3-(1-methyl-1*H*-indol-3-yl)-1-oxopropan-2-yl)amino)-4-methyl-1-oxopentan-2-aminium dihydrogen phosphate (**62-P**). Obtained in 59% yield. LCMS (ESI, m/z): 360.42 [M + H] $^+$. $^1\text{H NMR}$ (DMSO- d_6): δ 0.77 (dd, 6H, $J = 6.5, 6\text{H}, 2.2$ Hz), 1.1 (t, 3H, $J = 7.1, 7.1$ Hz), 1.18–1.32 (m, 1H), 1.39–1.50 (m, 1H), 1.39–1.49 (m, 1H), 3.06 (dd, 1H, $J = 14.5, 8.4$ Hz), 3.17 (dd, 1H, $J = 14.4, 5.4$ Hz), 3.40 (dd, 1H, $J = 8.6, 5.7$ Hz), 3.72 (s, 3H), 4.06 (q, 2H, $J = 7.1, 7.1, 7.1$ Hz), 4.55 (td, 1H, $J = 8.1, 8.1, 5.5$ Hz), 5.52 (bs, 8H), 7.02 (t, 1H, $J = 7.2$ Hz), 7.10–7.15 (m, 2H), 7.38 (d, 1H, $J = 8.3$ Hz), 7.51 (d, 1H, $J = 7.9$ Hz), 8.62 (d, 1H, $J = 7.9$ Hz).

4.1.15.7. (*S*)-1-(((*R*)-1-Ethoxy-3-(1-methyl-1*H*-indol-3-yl)-1-oxopropan-2-yl)amino)-4-(methylthio)-1-oxobutan-2-aminium dihydrogen phosphate (**64-P**). Obtained with 70% yield. $^1\text{H NMR}$ (DMSO- d_6): δ 1.13 (t, 3H, $J = 7.1$ Hz), 1.64–1.72 (m, 1H), 1.73–1.84 (m, 1H), 1.93 (s, 3H), 2.28 (t, 2H, $J = 7.9$ Hz), 3.08 (dd, 1H, $J = 14.6, 8.5$ Hz), 3.18 (dd, 1H, $J = 14.5, 5.2$ Hz), 3.54 (t, 1H, $J = 6.0$ Hz), 3.73 (s, 3H), 4.07 (q, 2H, $J = 7.1$ Hz), 4.56 (q, 1H, $J = 6.8, 6.1$ Hz), 7.02 (t, 1H, $J = 7.4$ Hz), 7.07–7.23 (m, 2H), 7.38 (d, 1H, $J = 8.2$ Hz), 7.51 (d, 1H, $J = 7.9$ Hz), 7.98 (br s, 5H), 8.68 (d, 1H, $J = 7.7$ Hz).

4.1.16. General method for the generation of mono and di methanesulfonate and benzenesulfonate salts of indoximod prodrugs

To a solution of each prodrug in its free base form (0.25 g, 0.723 mmol) in ethanol (10 mL) at rt, was added methanesulfonic or benzenesulfonic acid (0.723 mmol or 1.446 mmol in case of diamines) and the mixture was stirred at rt overnight. Ethanol was evaporated and the crude product was stirred in methyl *tert*-butyl ether for 1–5 h. The precipitate was filtered and dried to yield the corresponding methanesulfonate or benzenesulfonate salt.

4.1.16.1. (2*R*)-1-(2,3-Dihydroxypropoxy)-3-(1-methyl-1*H*-indol-3-yl)-1-oxopropan-2-aminium methanesulfonate (**8-M**). Obtained with 41% yield. $^1\text{H NMR}$ (DMSO- d_6): δ 2.31 (s, 3H), 3.24–3.29 (m, 2H), 3.29–3.41 (m, 2H), 3.65–3.68 (m, 1H), 3.75 (s, 3H), 4.04 (dd, 1H, $J = 11.1, 6.3$ Hz), 4.16 (dd, 1H, $J = 11.0, 4.0$ Hz), 4.28 (br s, 1H), 7.06 (ddd, 1H, $J = 8.0, 7.1, 1.0$ Hz), 7.17 (ddd, 1H, $J = 8.2, 7.1, 1.1$ Hz), 7.21 (s, 1H), 7.39–7.46 (m, 1H), 7.54 (dt, 1H, $J = 8.1, 0.9$ Hz), 8.29 (br s, 3H).

4.1.16.2. ((*S*)-5-Amino-1-(((*R*)-1-ethoxy-3-(1-methyl-1*H*-indol-3-yl)-1-oxopropan-2-yl)amino)-1,5-dioxopentan-2-aminium methanesulfonate (**59-M**). Obtained with 78% yield. $^1\text{H NMR}$ (DMSO- d_6): δ 1.11 (t, 3H, $J = 7.1$ Hz), 1.80–1.86 (m, 2H), 1.97–2.13 (m, 2H), 2.31 (s, 3H), 3.08 (dd, 1H, $J = 14.5, 8.2$ Hz), 3.18 (dd, 1H, $J = 14.5, 6.0$ Hz), 3.72 (s, 3H), 3.85 (q, 1H, $J = 5.6$ Hz), 4.06 (q, 2H, $J = 7.1$ Hz), 4.59 (td, 1H, $J = 8.0, 6.0$ Hz), 6.98 (s, 1H), 7.03 (ddd, 1H, $J = 8.0, 6.9, 1.0$ Hz), 7.09–7.18 (m, 2H), 7.34–7.42 (m, 2H), 7.52 (dt, 1H, $J = 7.9, 1.0$ Hz), 8.12 (d, 3H, $J = 5.6$ Hz), 8.93 (d, 1H, $J = 7.9$ Hz).

4.1.16.3. (*S*)-1-(((*R*)-1-Ethoxy-3-(1-methyl-1*H*-indol-3-yl)-1-oxopropan-2-yl)amino)-4-methyl-1-oxopentan-2-aminium methanesulfonate (**62-M**). It was obtained in 69% yield. LCMS (ESI, m/z): 360.42 [M + H] $^+$. $^1\text{H NMR}$ (DMSO- d_6): δ 0.73 (dd, 6H, $J = 8.2, 6.3$ Hz), 6H), 1.16 (t, 3H, $J = 7.1, 7.1$ Hz), 1.24 (t, 2H, $J = 7.1, 7.1$ Hz), 1.32 (dt, 1H, $J = 13.0, 6.7, 6.7$ Hz), 2.29 (s, 3H), 3.03 (dd, 1H, $J = 14.5, 9.3$ Hz), 3.20 (dd, 1H, $J = 14.5, 5.3$ Hz), 3.72 (s, 3H), 4.11 (q, 2H, $J = 7.1$ Hz), 4.64 (td, 1H, $J = 8.8, 5.5$ Hz), 7.02 (t, 1H, $J = 7.5$ Hz), 7.13 (d, 2H, $J = 9.8$ Hz), 7.38 (d, 1H, $J = 8.2$ Hz), 7.52 (d, 1H, $J = 7.9$ Hz), 8.01 (s, 3H), 8.92 (d, 1H, $J = 8.2$ Hz, 1H).

4.1.16.4. Ethyl N^{α} -((*S*)-2-(λ^4 -azanyl)-4-methylpentanoyl)-1-methyl-*D*-tryptophanate besylate (**62-B**). It was obtained in 68% yield. LCMS (ESI, m/z): 360.42 [M + H] $^+$. $^1\text{H NMR}$ (DMSO- d_6): δ 0.73 (dd, 6H, $J = 8.2, 6.3$ Hz), 1.16 (t, 3H, $J = 7.1$ Hz), 1.24 (t, 2H, $J = 7.3$ Hz), 1.32 (dt, 1H, $J = 13.0, 6.5$ Hz), 2.98–3.09 (m, 1H), 3.20 (dd, 1H, $J = 14.5, 5.2$ Hz), 3.72 (s, 3H), 4.11 (q, 2H, $J = 7.1$ Hz), 4.64 (td, 1H, $J = 8.9, 5.4$ Hz), 6.99–7.05 (m, 1H), 7.09–7.17 (m, 2H), 7.26–7.35 (m, 3H), 7.38 (d, 1H, $J = 8.2$ Hz), 7.52 (d, 1H, $J = 8.0$ Hz), 7.59 (dd, 2H, $J = 7.7, 1.9$ Hz), 8.00 (s, 3H), 8.92 (d, 1H, $J = 8.2$ Hz).

4.1.17. General method for the generation of mono, disulfate and hydrogen sulfate salts of indoximod and indoximod prodrugs

To a solution of each prodrug in its free base form (1.22 mmol) in dry THF (10 mL) at 0 °C was added sulfuric acid (0.611 mmol or 1.22 mmol) as a solution in THF (2 mL) and the solution was allowed to warm to rt. After stirring for 2–6 h, the solvent was distilled-off and the crude was stirred with methyl *tert*-butyl ether, the solid was filtered and dried under vacuum to yield the desired product.

4.1.17.1. (2*R*)-1-(2,3-Dihydroxypropoxy)-3-(1-methyl-1*H*-indol-3-yl)-1-oxopropan-2-aminium sulfate (**8-S**). Obtained with 43% yield. $^1\text{H NMR}$ (DMSO- d_6): δ 3.05–3.19 (m, 2H), 3.29–3.40 and 3.44–3.55 (two m, 2H), 3.62–3.69 (m, 1H), 3.74 (s, 3H), 3.89–3.99 (m, 2H), 4.07–4.12 (m, 1H), 6.25 (br s, 2H), 7.03 (t, 1H, $J = 7.7$ Hz), 7.11–7.21 (m, 2H), 7.40 (d, 1H, $J = 8.1$ Hz), 7.51–7.57 (m, 1H).

4.1.17.2. (*S*)-6-(((*R*)-1-Carboxy-2-(1-methyl-1*H*-indol-3-yl)ethyl)amino)-6-oxohexane-1,5-diaminium sulfate (**46-S**). Obtained with 82% yield. $^1\text{H NMR}$ (DMSO- d_6): δ 1.08–1.58 (m, 7H), 2.55–2.71 (m, 2H), 3.03 (dd, 1H, $J = 14.6, 8.8$ Hz), 3.21 (dd, 1H, $J = 14.6, 4.9$ Hz), 3.63 (s, 1H), 3.72 (s, 3H), 4.53 (d, 1H, $J = 7.9$ Hz), 7.02 (t, 1H, $J = 7.4$ Hz), 7.09–7.18 (m, 2H), 7.37 (d, 1H, $J = 8.2$ Hz), 7.56 (d, 1H, $J = 7.9$ Hz), 8.25 (br s, 6H).

4.1.17.3. (*S*)-5-Amino-1-(((*R*)-1-ethoxy-3-(1-methyl-1*H*-indol-3-yl)-1-oxopropan-2-yl)amino)-1,5-dioxopentan-2-aminium sulfate (**59-S**). Obtained with 83% yield. $^1\text{H NMR}$ (DMSO- d_6): δ 1.10 (t, 3H, $J = 7.1$ Hz), 1.63–1.74 (m, 1H), 1.75–1.86 (m, 1H), 2.02–2.07 (m, 2H), 3.13 (qd, 2H, $J = 14.5, 6.8$ Hz), 3.52 (dd, 1H, $J = 7.4, 5.0$ Hz), 3.72 (s, 3H), 4.04 (q, 2H, $J = 7.1$ Hz), 4.55 (q, 1H, $J = 1.6$ Hz), 6.47 (br s, 2H), 6.85 (s, 1H), 7.03 (t, 1H, $J = 7.5$ Hz), 7.10–7.19 (m, 2H), 7.29 (s, 1H), 7.38 (d, 1H, $J = 8.2$ Hz), 7.51 (d, 1H, $J = 7.9$ Hz), 8.59 (d, 1H, $J = 7.9$ Hz).

4.1.17.4. Ethyl N^{α} -((*S*)-2-(λ^4 -azanyl)-4-methylpentanoyl)-1-methyl-*D*-tryptophanate sulfate (**62-S**). Obtained with 29% yield. $^1\text{H NMR}$ (DMSO- d_6): δ 0.72–0.78 (m, 6H), 1.11 (t, 3H, $J = 7.2, 7.2$ Hz), 1.14–1.18 (m, 1H), 1.22–1.30 (m, 1H), 1.45 (dt, 1H, $J = 13.5, 6.8, 6.8$ Hz), 3.00–3.08 (m, 1H), 3.15 (dd, 1H, $J = 14.5, 5.6$ Hz), 3.70 (s, 3H), 4.05 (q, 2H, $J = 7.1, 7.1$ Hz), 4.54 (q, 1H, $J = 7.5, 7.5, 7.4$ Hz), 7.00 (t, 1H, $J = 7.5, 7.5$ Hz), 7.11 (m, 2H), 7.36 (d, 1H, $J = 8.2$ Hz), 7.49 (d, 1H, $J = 7.9$ Hz), 8.48 (d, 1H, $J = 7.9$ Hz).

4.2. Stability studies of prodrugs

Prodrugs were dissolved in DMSO at 200 μM and added to the test matrices at final concentration of 5 μM . An aliquot was immediately taken at $t = 0$, flash frozen in liquid nitrogen and stored at -80°C until analysis. The rest of the sample was incubated at 37°C for the indicated time periods, aliquots taken and frozen at -80°C . Analysis was performed by precipitating aliquots with 4 vol acetonitrile, centrifugation and followed by LC-MS/MS analysis using a specific analytical method for each compound. Matrix solutions were: 1) saline solution, 2) 0.1 N HCl (pH 1) in water, 3) PBS buffer pH 7.2, 4) Simulated Gastric Fluid (SGF): 2 mg/mL NaCl, 3.2 mg/mL pepsin, HCl to pH 1.2, 5) Simulated Intestinal Fluid (SIF): 6.8 mg/mL K_2HPO_4 , NaOH to pH 6.8 ($\sim 38\text{ mM}$), 10 mg/mL pancreatin.

For plasma stability measurements, 450 μL of plasma at 37°C was mixed with 50 μL of 50 μM solution of the test compound. Aliquots (50 μL) were taken at 0, 15, 30, 45, 60, 90 and 120 min and mixed with 4 vol of cold acetonitrile, centrifuged and analyzed by LC-MS/MS using a specific method for each prodrug. The relative concentrations (areas) were plotted vs time, and the percentage of area under the curve was used as a measure of the stability of each prodrug in plasma.

4.3. Pharmacokinetics

4.3.1. Preparation of capsules and PK in rats

When testing pharmacokinetics of indoximod after dosing different prodrugs in solution, prodrugs were formulated in either saline, Cremaphor®: EtOH: saline (10:10:80), or Chremaphor: EtOH: saline: HCl (10:10:80:0.1 N) at 2 mg/mL (mg of free base of each prodrug), dosed at 5 mL/kg to achieve a dose of 10 mg/kg.

To test PK in rats by dosing capsules, gelatin capsules (Torpac, 20 mg capacity) were manually prepared containing 11 μmol /capsule A, 28 μmol /capsule B or 50 μmol /capsule C of indoximod free base (2.5, 6.3 or 11.4 mg/capsule, respectively) or its prodrugs in their various salt forms, in an excipient blend consisting of microcrystalline cellulose, lactose monohydrate, croscarmellose sodium and magnesium stearate in the proportions shown in Table 1, Supplementary Methods. The composition and dose uniformity of a representative sample of capsules from each batch was verified by weight and by LC-MS/MS to determine the average indoximod or prodrug content. To test the pharmacokinetic profile achieved by dosing indoximod prodrugs in different salt forms, 1 capsule A (11 μmol /capsule) or 2 capsules B (28 μmol /capsule) or 3 capsules C (50 μmol /capsule) were dosed to rats by intra-stomach delivery.

Rats were fasted 16 h prior to dosing to eliminate any confounding food effects, and food was returned 2 h after dosing. Blood samples were obtained from each rat at 0, 15 min, 30 min, 1 h, 2 h, 4 h, 6 h, 10 h, 24 h, 48 h and 72 h after dosing. The concentration of indoximod in plasma was determined by LC-MS/MS, and pharmacokinetic parameters were calculated using the software WinNonLin (Certara). An individual set of pharmacokinetic parameters were calculated for each animal.

4.3.2. Preparation of capsules and PK in cynomolgus monkeys

For comparison of pharmacokinetics of indoximod with that of prodrugs **62-Cl** and **64-Cl**, the plasma pharmacokinetics of indoximod capsule and test formulations **62-Cl** and **64-Cl** capsules was studied following single oral administrations to male Cynomolgus monkeys in a crossover study design. Nine non-naïve male Cynomolgus monkeys were assigned to 3 treatment groups, and each group had three male animals. In this study with crossover design, the animals were dosed with indoximod, **62-Cl** or **64-Cl** capsules at

different dose levels. Each group orally was dosed at a different dose level. Group 1 animals were dosed with 1 Capsule A at the target dose of 92 $\mu\text{mol}/\text{kg}$; Group 2 animals were dosed with 3 Capsules A at the target dose of 275 $\mu\text{mol}/\text{kg}$ and Group 3 animals were dosed with 4 Capsules B at target dose of 825 $\mu\text{mol}/\text{kg}$. Capsule compositions are described in Table 2, Supplementary Materials. Blood samples were collected at pre-dose, 0.083, 0.25, 0.5, 1, 2, 4, 8, 12, 24, 36 and 48 h post-dose. Concentrations of indoximod in plasma samples were determined by LC-MS/MS.

For PK studies with **NLG802** and determination of oral bioavailability, a group of 3 males and 3 females were administered a single dose of 15 mg/kg **NLG802** (2 mL/kg of a 7.5 mg/mL) by intravenous (IV) injection, followed by blood collections up to 24 h post dose for pharmacokinetic analysis. Two weeks later, the same animals were dosed orally by nasal gastric gavage a single dose of 75 mg/kg, followed by blood collections up to 24 h post dose from all animals and urine and feces collections up to 12 h post dose for pharmacokinetic and excretion analysis. Additional groups of animals (3 males and 3 females per group) were dosed by nasal gastric gavage at 0, 225 and 675 mg/kg **NLG802**, followed by blood collection for 24 h. The concentration of the parent prodrug **62**, the intermediate metabolite M9 and the active metabolite indoximod were determined from plasma samples using a validated bio-analytical method. Pharmacokinetic parameters were calculated by non-compartmental analysis using WinNonLin software (Certara).

4.3.3. Metabolite identification in hepatocytes from different species

Metabolite identification of **NLG802** was conducted by incubation of 10 μM **NLG802** with hepatocytes from 5 different species (CD-1 mouse, Sprague Dawley rats, Beagle dogs, Cynomolgus monkey and human) at 37°C for 120 min, and samples analyzed by using UPLC-QTOF-PDA system. MetaboLynx™ software was used for the post-acquisition data processing and the structures of the metabolites were elucidated based on the characteristics of their MS and MS² data.

4.4. Antitumor activity

C57Bl/6 female mice, 8–10 weeks of age, weighing 20–25 g were inoculated with 10^5 B16F10 cells subcutaneously in the flank on Day 1. **NLG802** (99.7% purity), was formulated in 0.5% (w/v) HEC, 0.25% Tween 80 and 0.01% simethicone, in water, at 7.04, 14.06, 28.35 and 56.69 mg/mL, and administered by oral gavage at 0.2 mL per animal, twice a day, from days 6–11. Spleen cells for pmel-1 mice [55] were harvested, made into simple cell suspension by using mesh, sorted by magnetic beads using EasySep Mouse CD8⁺T cell isolation kit (StemCell Technologies). Purified CD8⁺ T cells were injected intravenously by tail vein injection at 2×10^6 T cells per mouse, on Day 7. Vaccination to stimulate adoptively transferred pmel-1 cells was performed as described [56]. Briefly, an emulsion of gp100 peptide (synthesized by HP Chemicals, sequence KVPRNQDWL, 25 μg) and CpG ODN (from TriLink Biotechnologie Inc, 5' TCC ATG ACG TTC CTG ACG TT 3', 50 μg), and IFA was made with use of two-way syringes. Vaccine in total volume of 50 μL (containing 25 μg gp100 peptide and 50 μg CpG ODN) was injected into the foot pad of experimental mice on the same side as the established tumor, once on Day 7. Tumors were measured with caliper on Day 11 and tumor volume was calculated by multiplying the dimensions of the tumor.

Declaration of competing interest

The authors declare that they have no known competing financial interests or personal relationships that could have

appeared to influence the work reported in this paper.

Appendix A. Supplementary data

Supplementary data to this article can be found online at <https://doi.org/10.1016/j.ejmech.2020.112373>.

References

- [1] D.H. Munn, A.L. Mellor, Ido in the tumor microenvironment: inflammation, counter-regulation, and tolerance, *Trends Immunol.* 37 (2016) 193–207.
- [2] J.E. Honig, J.C. Osborne, S.T. Nichol, Crimean-Congo hemorrhagic fever virus genome L RNA segment and encoded protein, *Virology* 321 (2004) 29–35.
- [3] B. Baban, P. Chandler, D. McCool, B. Marshall, D.H. Munn, A.L. Mellor, Indoleamine 2,3-dioxygenase expression is restricted to fetal trophoblast giant cells during murine gestation and is maternal genome specific, *J. Reprod. Immunol.* 61 (2004) 67–77.
- [4] D.H. Munn, M. Zhou, J.T. Attwood, I. Bondarev, S.J. Conway, B. Marshall, C. Brown, A.L. Mellor, Prevention of allogeneic fetal rejection by tryptophan catabolism, *Science* 281 (1998) 1191–1193.
- [5] A.L. Mellor, P. Chandler, G.K. Lee, T. Johnson, D.B. Keskin, J. Lee, D.H. Munn, Indoleamine 2,3-dioxygenase, immunosuppression and pregnancy, *J. Reprod. Immunol.* 57 (2002) 143–150.
- [6] C. Uyttenhove, L. Pilotte, I. Theate, V. Stroobant, D. Colau, N. Parmentier, T. Boon, B.J. Van den Eynde, Evidence for a tumoral immune resistance mechanism based on tryptophan degradation by indoleamine 2,3-dioxygenase, *Nat. Med.* 9 (2003) 1269–1274.
- [7] A.J. Muller, J.B. DuHadaway, P.S. Donover, E. Sutanto-Ward, G.C. Prendergast, Inhibition of indoleamine 2,3-dioxygenase, an immunoregulatory target of the cancer suppression gene Bin1, potentiates cancer chemotherapy, *Nat. Med.* 11 (2005) 312–319.
- [8] A. Okamoto, T. Nikaido, K. Ochiai, S. Takakura, M. Saito, Y. Aoki, N. Ishii, N. Yanaihara, K. Yamada, O. Takikawa, R. Kawaguchi, S. Isonishi, T. Tanaka, M. Urashima, Indoleamine 2,3-dioxygenase serves as a marker of poor prognosis in gene expression profiles of serous ovarian cancer cells, *Clin. Canc. Res.* 11 (2005) 6030–6039.
- [9] G. Weinelich, C. Murr, L. Richardsen, C. Winkler, D. Fuchs, Decreased serum tryptophan concentration predicts poor prognosis in malignant melanoma patients, *Dermatology (Basel)* 214 (2007) 8–14.
- [10] W. Wang, L. Huang, J.Y. Jin, S. Jolly, Y. Zang, H. Wu, L. Yan, W. Pi, L. Li, A.L. Mellor, F.S. Kong, Ido immune status after chemoradiation may predict survival in lung cancer patients, *Canc. Res.* 78 (2018) 809–816.
- [11] M. Hoshi, H. Ito, H. Fujigaki, M. Takemura, T. Takahashi, E. Tomita, M. Ohyama, R. Tanaka, K. Saito, M. Seishima, Indoleamine 2,3-dioxygenase is highly expressed in human adult T-cell leukemia/lymphoma and chemotherapy changes tryptophan catabolism in serum and reduced activity, *Leuk. Res.* 33 (2009) 39–45.
- [12] A. Witkiewicz, T.K. Williams, J. Cozzitorto, B. Durkan, S.L. Showalter, C.J. Yeo, J.R. Brody, Expression of indoleamine 2,3-dioxygenase in metastatic pancreatic ductal adenocarcinoma recruits regulatory T cells to avoid immune detection, *J. Am. Coll. Surg.* 206 (2008) 849–854, discussion 854–846.
- [13] M. Takao, A. Okamoto, T. Nikaido, M. Urashima, S. Takakura, M. Saito, S. Okamoto, O. Takikawa, H. Sasaki, M. Yasuda, K. Ochiai, T. Tanaka, Increased synthesis of indoleamine-2,3-dioxygenase protein is positively associated with impaired survival in patients with serous-type, but not with other types of, ovarian cancer, *Oncol. Rep.* 17 (2007) 1333–1339.
- [14] G. Brandacher, A. Perathoner, R. Ladurner, S. Schneeberger, P. Obrist, C. Winkler, E.R. Werner, G. Werner-Felmayer, H.G. Weiss, G. Gobel, R. Margreiter, A. Konigsrainer, D. Fuchs, A. Amberger, Prognostic value of indoleamine 2,3-dioxygenase expression in colorectal cancer: effect on tumor-infiltrating T cells, *Clin. Canc. Res.* 12 (2006) 1144–1151.
- [15] J.R. Lee, R.R. Dalton, J.L. Messina, M.D. Sharma, D.M. Smith, R.E. Burgess, F. Mazzella, S.J. Antonia, A.L. Mellor, D.H. Munn, Pattern of recruitment of immunoregulatory antigen-presenting cells in malignant melanoma, *Laboratory investigation* 83 (2003) 1457–1466.
- [16] I. Theate, N. van Baren, L. Pilotte, F. Moulin, P. Larrieu, J.C. Renauld, C. Herve, I. Gutierrez-Roelens, E. Marbaix, C. Sempoux, B.J. Van den Eynde, Extensive profiling of the expression of the indoleamine 2,3-dioxygenase 1 protein in normal and tumoral human tissues, *Canc. Immunol Res* 3 (2015) 161–172.
- [17] C.A. Opitz, U.M. Litzenburger, F. Sahn, M. Ott, I. Tritschler, S. Trump, T. Schumacher, L. Jestaedt, D. Schrenk, M. Weller, M. Jugold, G.J. Guillemin, C.L. Miller, C. Lutz, B. Radlwimmer, I. Lehmann, A. von Deimling, W. Wick, M. Platten, An endogenous tumour-promoting ligand of the human aryl hydrocarbon receptor, *Nature* 478 (2011) 197–203.
- [18] L. Pilotte, F. Larrieu, V. Stroobant, D. Colau, E. Dolusic, R. Frederick, E. De Plaen, C. Uyttenhove, J. Wouters, B. Masereel, B.J. Van den Eynde, Reversal of tumoral immune resistance by inhibition of tryptophan 2,3-dioxygenase, *Proc. Natl. Acad. Sci. U. S. A.* 109 (2012) 2497–2502.
- [19] W. Peng, L. Robertson, J. Gallinetti, P. Mejia, S. Vose, A. Charlip, T. Chu, J.R. Mitchell, Surgical stress resistance induced by single amino acid deprivation requires Gcn2 in mice, *Sci. Transl. Med.* 4 (2012) 118ra111.
- [20] D.H. Munn, M.D. Sharma, B. Baban, H.P. Harding, Y. Zhang, D. Ron, A.L. Mellor, GCN2 kinase in T cells mediates proliferative arrest and anergy induction in response to indoleamine 2,3-dioxygenase, *Immunity* 22 (2005) 633–642.
- [21] R. Metz, S. Rust, J.B. Duhadaway, M.R. Mautino, D.H. Munn, N.N. Vahanian, C.J. Link, G.C. Prendergast, Ido inhibits a tryptophan sufficiency signal that stimulates mTOR: a novel Ido effector pathway targeted by D-1-methyl-tryptophan, *Oncolimmunology* 1 (2012) 1460–1468.
- [22] Q. Li, J.L. Harden, C.D. Anderson, N.K. Egilmez, Tolerogenic phenotype of IFN-gamma-induced Ido+ dendritic cells is maintained via an autocrine Ido-kynurenine/AhR-Ido loop, *J. Immunol.* 197 (2016) 962–970.
- [23] L.F. Ambrosio, C. Insfran, X. Volpini, E. Acosta Rodriguez, H.M. Serra, F.J. Quintana, L. Cervi, C.C. Motran, Role of aryl hydrocarbon receptor (AhR) in the regulation of immunity and immunopathology during trypanosoma cruzi infection, *Front. Immunol.* 10 (2019) 631.
- [24] C. Gutierrez-Vazquez, F.J. Quintana, Regulation of the immune response by the aryl hydrocarbon receptor, *Immunity* 48 (2018) 19–33.
- [25] F.J. Quintana, D.H. Sherr, Aryl hydrocarbon receptor control of adaptive immunity, *Pharmacol. Rev.* 65 (2013) 1148–1161.
- [26] J.D. Mezrich, J.H. Fechner, X. Zhang, B.P. Johnson, W.J. Burlingham, C.A. Bradford, An interaction between kynurenine and the aryl hydrocarbon receptor can generate regulatory T cells, *J. Immunol.* 185 (2010) 3190–3198.
- [27] W. Julliard, J.H. Fechner, J.D. Mezrich, The aryl hydrocarbon receptor meets immunology: friend or foe? A little of both, *Front. Immunol.* 5 (2014) 458.
- [28] N.T. Nguyen, A. Kimura, T. Nakahama, I. Chinen, K. Masuda, K. Nohara, Y. Fujii-Kuriyama, T. Kishimoto, Aryl hydrocarbon receptor negatively regulates dendritic cell immunogenicity via a kynurenine-dependent mechanism, *Proc. Natl. Acad. Sci. U. S. A.* 107 (2010) 19961–19966.
- [29] E.L. Brincks, J. Adams, M. Essmann, B.A. Turner, L. Wang, J. Ke, A. Marciniowicz, N. Vahanian, C. Link Jr., M.R. Mautino, Indoximod modulates AhR-driven transcription of genes that control immune function, *Canc. Res.* 78 (2018).
- [30] H.H. Soliman, E. Jackson, T. Neuger, E.C. Dees, R.D. Harvey, H. Han, R. Ismail-Khan, S. Minton, N.N. Vahanian, C. Link, D.M. Sullivan, S. Antonia, A first in man phase I trial of the oral immunomodulator, indoximod, combined with docetaxel in patients with metastatic solid tumors, *Oncotarget* 5 (2014) 8136–8146.
- [31] H.H. Soliman, S.E. Minton, H.S. Han, R. Ismail-Khan, A. Neuger, F. Khambati, D. Noyes, R. Lush, A.A. Chiappori, J.D. Roberts, C. Link, N.N. Vahanian, M. Mautino, H. Streicher, D.M. Sullivan, S.J. Antonia, A phase I study of indoximod in patients with advanced malignancies, *Oncotarget* 7 (2016) 22928–22938.
- [32] D.K. Kim, N. Lee, Y.W. Kim, K. Chang, G.J. Im, W.S. Choi, K.H. Kim, Synthesis and evaluation of amino acid esters of 6-deoxy penciclovir as potential prodrugs of penciclovir, *Bioorg. Med. Chem.* 7 (1999) 419–424.
- [33] M.D. Pescovitz, J. Rabkin, R.M. Merion, C.V. Paya, J. Pirsch, R.B. Freeman, J. O'Grady, C. Robinson, Z. To, K. Wren, L. Banken, W. Buhles, F. Brown, Valganciclovir results in improved oral absorption of ganciclovir in liver transplant recipients, *Antimicrob. Agents Chemother.* 44 (2000) 2811–2815.
- [34] X. Song, B.S. Vig, P.L. Lorenzi, J.C. Drach, L.B. Townsend, G.L. Amidon, Amino acid ester prodrugs of the antiviral agent 2-bromo-5,6-dichloro-1-(beta-D-ribofuranosyl)benzimidazole as potential substrates of hPEPT1 transporter, *J. Med. Chem.* 48 (2005) 1274–1277.
- [35] A.M.S. M. S. Mandekar, S. Desikan, T. Ramar, L. Subramani, M. Annadurai, S.D. Desai, S. Sinha, S.M. Jenkins, M.R. Krystal, M. Subramanian, S. Sridhar, S. Padmanabhan, P. Bhutani, R. Arla, S. Singh, J. Sinha, M. Thakur, J.F. Kadow, N.A. Meanwell, Design, synthesis, and pharmacokinetic evaluation of phosphate and amino acid ester prodrugs for improving the oral bioavailability of the HIV-1 protease inhibitor atazanavir, *J. Med. Chem.* 62 (2019) 3553–3574.
- [36] A. Diez-Torrubia, S. Cabrera, S. de Castro, C. Garcia-Aparicio, G. Mulder, I. De Meester, M.J. Camarasa, J. Balzarini, S. Velazquez, Novel water-soluble prodrugs of acyclovir cleavable by the dipeptidyl-peptidase IV (DPP IV/CD26) enzyme, *Eur. J. Med. Chem.* 70 (2013) 456–468.
- [37] M. Gooyit, M. Lee, V.A. Schroeder, M. Ikejiri, M.A. Suckow, S. Mobashery, M. Chang, Selective water-soluble gelatinase inhibitor prodrugs, *J. Med. Chem.* 54 (2011) 6676–6690.
- [38] I. Hutchinson, S.A. Jennings, B.R. Vishnuvajjala, A.D. Westwell, M.F. Stevens, Antitumor benzothiazoles. 16. Synthesis and pharmaceutical properties of antitumor 2-(4-aminophenyl)benzothiazole amino acid prodrugs, *J. Med. Chem.* 45 (2002) 744–747.
- [39] K.C. Lee, E. Venkateswararao, V.K. Sharma, S.H. Jung, Investigation of amino acid conjugates of (S)-1-[1-(4-aminobenzoyl)-2,3-dihydro-1H-indol-6-sulfonyl]-4-phenyl-imidazolidin-2-one (DW2282) as water soluble anti-cancer prodrugs, *Eur. J. Med. Chem.* 80 (2014) 439–446.
- [40] N.L. Pochopin, W.N. Charman, V.J. Stella, Pharmacokinetics of dapsone and amino acid prodrugs of dapsone, *Drug Metab. Dispos.* 22 (1994) 770–775.
- [41] A. Guo, P. Hu, P.V. Balimane, F.H. Leibach, P.J. Sinko, Interactions of a non-peptidic drug, valacyclovir, with the human intestinal peptide transporter (hPEPT1) expressed in a mammalian cell line, *J. Pharmacol. Exp. Therapeut.* 289 (1999) 448–454.
- [42] C.P. Landowski, B.S. Vig, X. Song, G.L. Amidon, Targeted delivery to PEPT1-overexpressing cells: acidic, basic, and secondary floxuridine amino acid ester prodrugs, *Mol. Canc. Therapeut.* 4 (2005) 659–667.
- [43] B. Steffansen, C.U. Nielsen, B. Brodin, A.H. Eriksson, R. Andersen, S. Frokjaer, Intestinal solute carriers: an overview of trends and strategies for improving oral drug absorption, *Eur. J. Pharmaceut. Sci.* 21 (2004) 3–16.
- [44] C.R. Santos, R. Capela, C.S. Pereira, E. Valente, L. Gouveia, C. Panecouque, E. De Clercq, R. Moreira, P. Gomes, Structure-activity relationships for dipeptide

- prodrugs of acyclovir: implications for prodrug design, *Eur. J. Med. Chem.* 44 (2009) 2339–2346.
- [45] N. Vale, A. Ferreira, J. Matos, P. Fresco, M.J. Gouveia, Amino acids in the development of prodrugs, *Molecules* 23 (2018).
- [46] N. Vale, F. Nogueira, V.E. do Rosario, P. Gomes, R. Moreira, Primaquine dipeptide derivatives bearing an imidazolidin-4-one moiety at the N-terminus as potential antimalarial prodrugs, *Eur. J. Med. Chem.* 44 (2009) 2506–2516.
- [47] E.M. del Amo, A. Urtti, M. Yliperttula, Pharmacokinetic role of L-type amino acid transporters LAT1 and LAT2, *Eur. J. Pharmaceut. Sci.* 35 (2008) 161–174.
- [48] A. Yamamoto, S. Akanuma, M. Tachikawa, K. Hosoya, Involvement of LAT1 and LAT2 in the high- and low-affinity transport of L-leucine in human retinal pigment epithelial cells (ARPE-19 cells), *J. Pharmacol. Sci.* 99 (2010) 2475–2482.
- [49] H.K. Han, D.M. Oh, G.L. Amidon, Cellular uptake mechanism of amino acid ester prodrugs in Caco-2/hPEPT1 cells overexpressing a human peptide transporter, *Pharm. Res. (N. Y.)* 15 (1998) 1382–1386.
- [50] G.M. Friedrichsen, W. Chen, M. Begtrup, C.P. Lee, P.L. Smith, R.T. Borchardt, Synthesis of analogs of L-valacyclovir and determination of their substrate activity for the oligopeptide transporter in Caco-2 cells, *Eur. J. Pharmaceut. Sci.* 16 (2002) 1–13.
- [51] B. Yang, D.E. Smith, Significance of peptide transporter 1 in the intestinal permeability of valacyclovir in wild-type and PepT1 knockout mice, *Drug Metab. Dispos.* 41 (2013) 608–614.
- [52] A.A. Patchett, The chemistry of enalapril, *Br. J. Clin. Pharmacol.* 18 (Suppl 2) (1984) 201S–207S.
- [53] N. Yumibe, K. Huie, K.J. Chen, M. Snow, R.P. Clement, M.N. Cayen, Identification of human liver cytochrome P450 enzymes that metabolize the non-sedating antihistamine loratadine. Formation of descarboethoxyloratadine by CYP3A4 and CYP2D6, *Biochem. Pharmacol.* 51 (1996) 165–172.
- [54] K. McClellan, C.M. Perry, Oseltamivir: a review of its use in influenza, *Drugs* 61 (2001) 263–283.
- [55] W.W. Overwijk, M.R. Theoret, S.E. Finkelstein, D.R. Surman, L.A. de Jong, F.A. Vyth-Dreese, T.A. DelleMijn, P.A. Antony, P.J. Spiess, D.C. Palmer, D.M. Heimann, C.A. Klebanoff, Z. Yu, L.N. Hwang, L. Feigenbaum, A.M. Kruisbeek, S.A. Rosenberg, N.P. Restifo, Tumor regression and autoimmunity after reversal of a functionally tolerant state of self-reactive CD8+ T cells, *J. Exp. Med.* 198 (2003) 569–580.
- [56] M.D. Sharma, L. Huang, J.H. Choi, E.J. Lee, J.M. Wilson, H. Lemos, F. Pan, B.R. Blazar, D.M. Pardoll, A.L. Mellor, H. Shi, D.H. Munn, An inherently bifunctional subset of Foxp3+ T helper cells is controlled by the transcription factor eos, *Immunity* 38 (2013) 998–1012.